Geothermal mining

The potential for environmentally friendly extraction of valuable components from geothermal brines in the Netherlands.

Bsc Minor Project

Maria Erica Biagini

Delft University of Technology

TU Delft

Geothermal mining

The potential for environmentally friendly extraction of valuable components from geothermal brines in the Netherlands.

by

Maria Erica Biagini

Student Name	Student Number
Maria Erica Biagini	5156688

Supervisors:	Ahmed Hussain
	Karl-Heinz Wolf
	Masoud Soleymani Shishvan
	David Bruhn
In collaboration with:	Pieter Bruijnen, EBN
Institution:	Delft University of Technology
Place:	Faculty of Civil Engineering and Geosciences, Delft
Project Duration:	January 2022 - August 2022

Cover Image: Gabbro Geothermal power plant in Larderello (PI), Italy by Vittorio Cucini (2021)

TU Delft

Disclaimer

This report holds public information available through companies and websites. The data were given under these conditions, and we do not take responsibility for the quality of the data provided.

Abstract

In a world transitioning towards renewable energies and lithium-battery powered cars, there has been an annual increase in demand of 6% for lithium and other rare metals between 2000 and 2008 (Stringfellow & Dobson, 2021a), and this increase in demand is forecast to continue through 2040 (Latnussa et al., 2020). Meanwhile, there is a concern that supply will not be able to keep up with demand. Most of the lithium in the European markets comes from other countries such as Chile and Australia, making the European lithium supply vulnerable to supply chain disruptions, as was observed during the COVID-19 pandemic (Latnussa et al., 2020). In addition, the economic value of lithium has increased more than threefold compared in 2022 compared to 2017 (Latnussa et al., 2022).

The geological information of Northern-Western Europe at the latest stage, gives an explanation to the occurrence of lithium in the Netherlands.

50 water samples of 13 fields are considered for the chemical composition and origin of their brine. All geothermal brines contain dissolved lithium and other metals from the reservoir formation and surroundings, allowing for metal 'mining' in an environmentally friendly manner. The highest lithium concentrations in aquifer brines are in the province of Drenthe and Limburg, specifically in the Akkrum-13 gas field (47-48 ppm) and the Californie Geothermie (20-28 ppm). The correlation is positive only for lithium against rubidium and lithium against the vicinity of volcanic intrusions, from mineral mobilization through groundwater flow. There are no specific formations with high lithium concentrations.

In Germany, construction has started on a project to extract lithium from geothermal process water, indicating that it is economically viable (Wedin, 2022). For the Netherlands there are 5 different surface options to extract the highest lithium concentrations. Reverse osmosis, nanofiltration, ion-exchange, sorbents and electrodialysis can be used as direct lithium extraction methodologies. One potential economical method to extract lithium from geothermal brines is by utilizing two centralized lithium extraction plants. A plant for the direct lithium extraction with ion-exchange resins, placed before injection wells, and one for the refinement of the material.

Table of Contents

List of Figures

Nomenclature

Abbreviations

Abbreviation	Definition
ISA	International Standard Atmosphere
CRM	Critical Raw Materials
EU	European Union
U.S.A.	United States of America
RO	Reverse Osmosis
NF	Nano Filtration
ED	Electrodialysis
FID	Final Investment Decision
DLE	Direct Lithium Extraction
M	Million
CPF	Central Processing Facility

Symbols

Symbol	Definition	Unit
ρ	Density	[kg/m^3]
A	Area	[m^2]
μ	Dynamic viscosity	[Pa·s]
L	Length	[m]
k	Permeability	[m^2]
P	Pressure	[Pa]
ΔP	Pressure differential	[Pa]
Q	Flow rate	[m^3/h]
T	Temperature	[°C]
R	Recovery	[%]
C	Concentration	[ppm or g/kg]
C_f	Feed concentration	[ppm or g/kg]
C_p	Permeate concentration	[ppm or g/kg]
V	Volume	[m^3]
R	Rejection or retention rate	[%]
j	Electrical current density	[A]

1

Introduction

a. Issue of the absence of metals (Li) for the energy transition

Lithium plays a crucial role in the energy transition (Flexer et al., 2018). Renewable energies are now in the spotlight of European governments and companies, to secure a future with a stable climate. Since the emission of carbon dioxide and other greenhouse gases, the transition to energy sources with lower emissions is the aim of European countries (Latunussa et al., 2020).

These 'greener' energy sources, such as solar and wind energy, require raw materials and 'rare' metals to meet the global demand that increased from 70,000 tons in 2020 to 93,000 tons in 2021 (U.S. Geological Survey, 2022). Electric energy storage, of which the transportation industry is a main driver of growth (Stringfellow & Dobson, 2021a), is based on lithium-ion batteries. Since lithium has a high charge density and the highest electrochemical potential of all metals, leading to high energy storage capacity (Liu et al., 2016).

The European Union (EU) imported 87% of the total lithium ore processed in the period between 2012 and 2016 (Latunussa et al., 2020). The EU imports 78% of its lithium ore from Chile and it predicted that the lithium supply will fall behind demand by 2030, thus it recognized the metal as Critical Raw Material (CRM). Therefore, the EU should be producing and extracting CRM from other (EU) sources, among others: geothermal brines and oil waste waters metals (Latunussa et al., 2020).

b. Case studies and metal production from geothermal brines

Pilot plants for lithium extraction from aquifer brines are in operation in the U.S.A. and Europe (Wedin, 2022 and E3 Metals Corp, 2021).

The largest lithium resource in Europe is in the Upper Rhine Graben (Germany) (Wedin, 2022). A series of geothermal plants already received the production license for lithium extraction in the area. The production well of Landau is already extracting lithium from geothermal brines in a pilot plant.

In the U.S.A. pilot plants have been constructed for the extraction of lithium and other metals such as zinc from the Salton Sea geothermal operations, to increase the profits of geothermal power plants ("Salton Sea Simbol Materials", n.d. [website]).

Moreover, other companies are investing to find new solutions to extract lithium from brines. An American oil company agreed on investing $6.35 million in a junior company that has developed a technology to extract lithium from the groundwater brine (Lee, 2022).

c. Research objectives and organization of this report

Here we investigate Dutch aquifers' water composition and lithium concentrations, the possible sources of lithium, and the extraction of lithium from geothermal brines. This report is organized as follows: in chapter 2 we discuss the theory of mineral formation and transportation. Chapter 3

contains the lithium sources from a literature study and the data retrieved whereas chapter 4 discusses the results of the findings. It is considered the possibility to recognize the presence of lithium from the correlation with other minerals or specific formations as well as the mobilization from other lithium sources. Chapter 5 investigates some advanced methodologies for lithium extraction from brines, two ongoing projects for extraction of lithium from aquifer brines. Finally, in chapter 6 can be found some suggestions to extract lithium in the Dutch subsurface.

2

Theory

Here we discuss the formation of minerals, the relevant geological history of North-West of Europe later on concentrating on the Netherlands and the theory of transport of minerals in the subsurface.

2.1. Mineral formations

Minerals form when atoms organize in lattice structures to form a solid substance (Grotzinger & Jordan, 2004). They can form in four different processes: from crystallization of a melt, from the results of sedimentation processes, because of metamorphism or due to chemical precipitation.

2.1.1. Formation processes

In igneous conditions, minerals form when elements in the magma re-arrange in a more ordered structure when the external temperature lowers. The fluid magma solidifies, and elements rearranges into crystalline ordered structures that are called minerals. Depending on the elements dissolved in the magma and the structures they form they are characterized as different minerals.
Sedimentary minerals form when rocks are subjected to weathering or erosion.
During metamorphic processes, where rocks undergo high temperature and pressures, the elements in the minerals re-arrange in different structures, generating different minerals.
Chemical precipitation occurs when the concentration of one compound exceeds its solubility. Minerals can precipitate due to the change in temperatures and changes in equilibrium reactions.

2.2. Relevant geological history: volcanism in the North-West of Europe and Netherlands

Late Carboniferous and Early Permian Volcanism

During the Variscan orogeny, from Late Carboniferous to Early Permian, tectonic movements caused a series of faults and vulcanism in the Dutch soil and surrounding North-West Europe (Wong, Batjes & de Jager, 2007).
The volcanism and intrusive activity of the latest Carboniferous can be seen in Figure 2.1 and extends from the Oslo Graben to the north of Midland Valley of Scotland, the North Sea, the Ringkøbing-Fin and the northern Germany (Doornenbal & Stevenson, 2010).

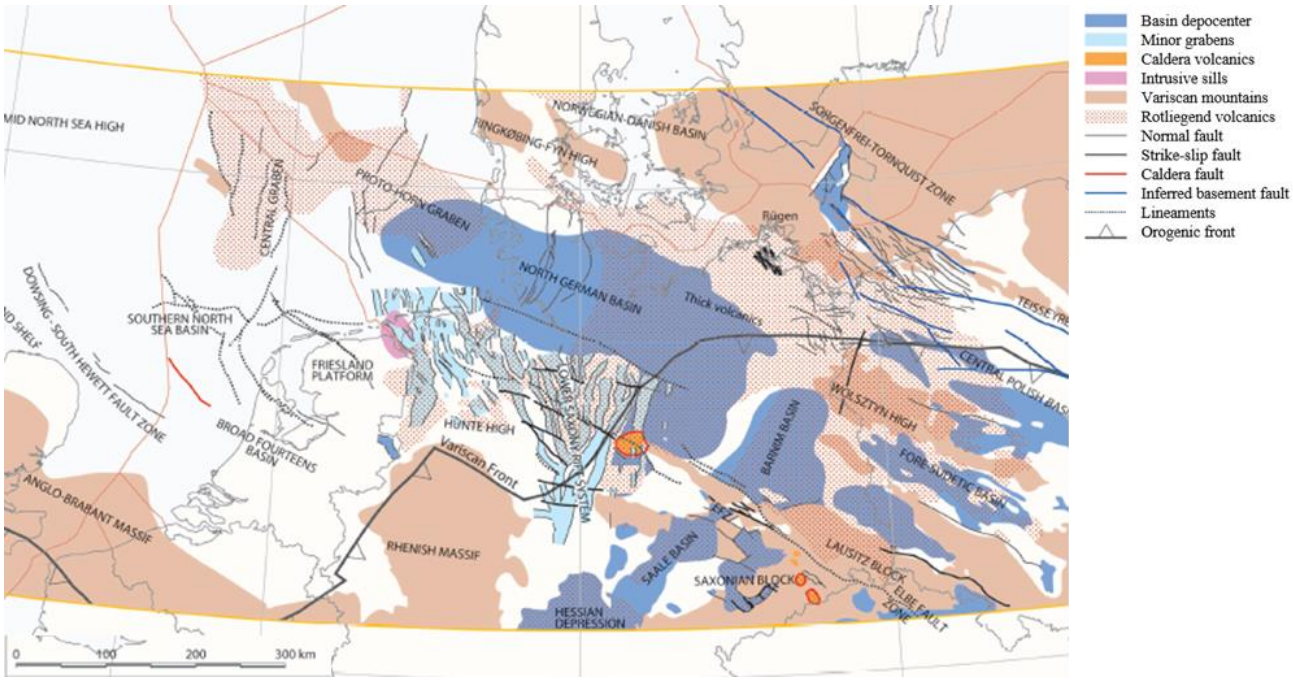

Figure 2.1: Tectonic evolution of the lower Rotliegend during Late Carboniferous and Early Permian (Doornenbal & Stevenson, 2010).

Another research from Wong et al. (2007) focused on the Dutch subsurface. They show that most of the rocks from that volcanism age are intrusive. The oldest volcanisms are found in some of the offshore fields, where a series of faults running through the central graben run also along the offshore fields K03, K04, P05 and P10, as can be seen from Figure 2.2. The volcanism, shown from Figure 2.1, is part of the Rotliegend volcanism.
Figure 2.1 and Figure 2.2 show higher tectonic activity and amount of intrusion is close to the Variscan Front, close to the German border. Together with the Rotliegend volcanism, some inferred intrusions are present: the Groningen and the Erkelenz intrusion.

Late Jurassic Volcanism

From Late Jurassic the extension of the North Sea graben, preceded by the uplifting of the North Sea, accelerated (Schroot, 1991). The rifting and subsidence were the cause to the Zuidwal volcanic complex developed in the Vlieland Basin.
The major volcanic feature is the Zuidwal Volcano, between Harlingen and Vlieland. The magma may have reached the surface along some reactivated faults that reopened during the extension on the graben. Other Jurassic intrusions were found in E6-1 well, offshore. The rocks identified in the K03, K04, P05, P10 and E6 field are biotite pyroxenites and tuff (Wong, et al., 2007).

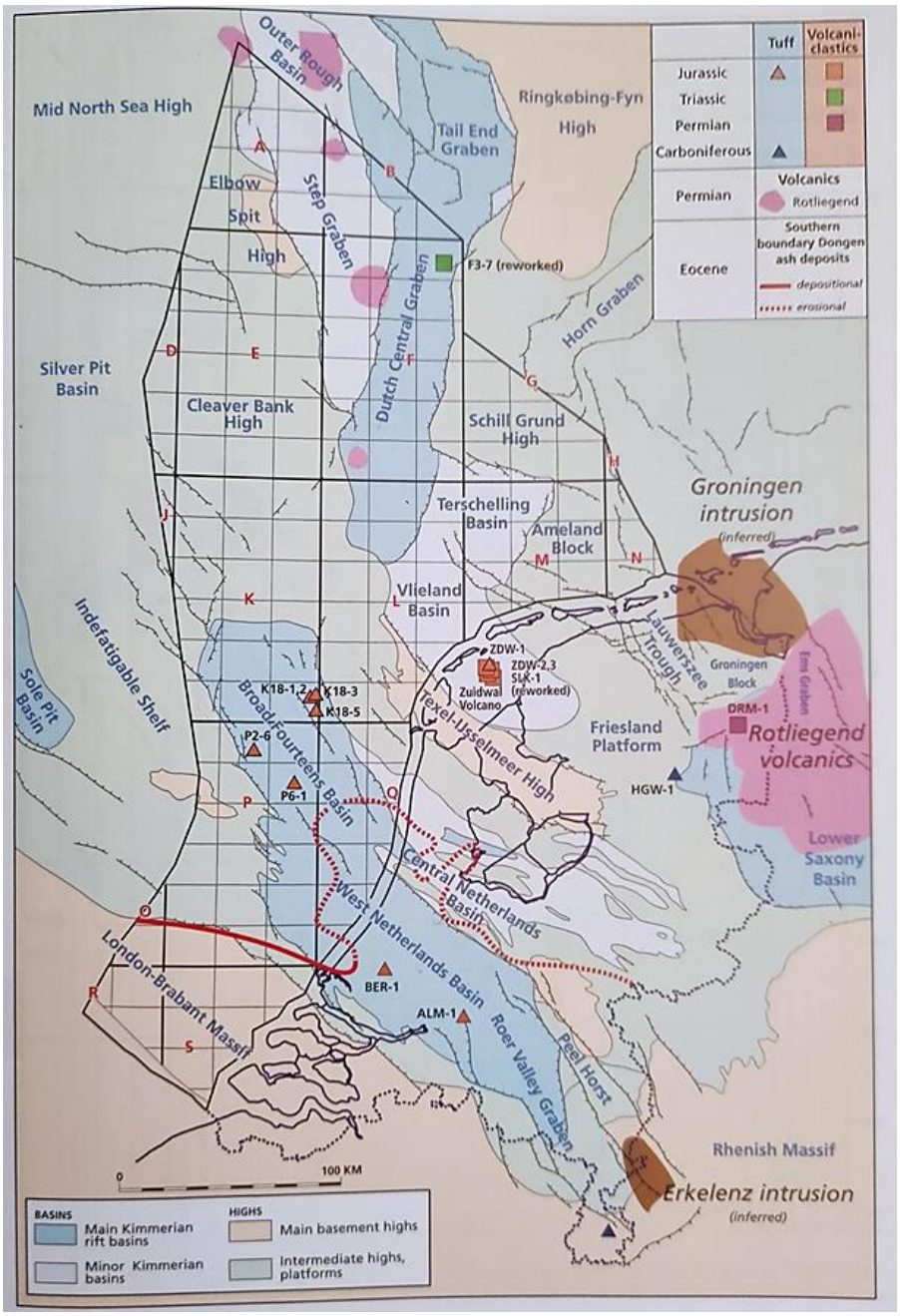

Figure 2.2: Map of the Netherlands showing the major volcanisms and borehole locations (Wong et al., 2007).

2.3. Transportation of minerals

The mineral composition of the groundwater is a result of chemical reactions and equilibrium states reached between the water and the gas as wells as the water and the solid rocks present in the subsurface (Mercado & Billings, 1975).

Dissolved minerals in a subsurface fluid body interact with the solid and gas interfaces at different ground temperatures, resulting in chemical reactions and equilibrium states. The fluids, moving through the pores, transport the minerals dissolved to different locations (Grotzinger & Jordan, 2004). This chapter is focused on three main transportation processes: magmatic intrusions, hydrothermal activities, and mineral dissolution in groundwater.

2.3.1. Magmatic intrusions

During tectonic activities magma can move through the Earth's crust until the shallower part of the subsurface. Magma, rich of elements from the asthenosphere, cools down slowly in the subsurface, allowing some crystals to grow and crystallize, thereby forming minerals such as pegmatites (Grotzinger & Jordan, 2004).

2.3.2. Hydrothermal activities

In tectonically active zones, the groundwater in contact with hot magmatic intrusions forms a hydrothermal solution that, in contact with the molten body, reacts with it. The resulting solution is enriched in elements from the magmatic intrusion. The resulting solution may move within the subsurface to cooler regions, where some minerals may precipitate (Grotzinger & Jordan, 2004).

2.3.3. Mineral transportation by groundwater

Dissolution

The chemical compounds present in the subsurface all behave to reach an equilibrium state determined by the equilibrium constant of the chemical reaction between the compounds. When groundwater flowing through the subsurface meets other solid rock or a fluid with another composition, chemical reactions occur until the system is again in equilibrium. The equilibrium constants of the chemical reactions at the subsurface conditions determine if reactions occur and if some elements dissolves in the water or not (Manahan, S., 1994).

Regardless the value of the equilibrium constant, it does not describe the speed and rate of reaction (Manahan, S., 1994). The rate of reaction, if the reaction is a dissolution of elements in the groundwater, is of relevant importance for this research. Depending on the dissolution rate, some elements in the contact body are present in higher concentrations than others.

The groundwater in the subsurface contains chemical compounds such as carbonic acid (H_2CO_3) and oxygen that are highly reactive with some elements of the solid rock, thereby possibly increasing the dissolution rate. Some minerals have higher dissolution rates than others, depending on the chemical stability between the mineral and the fluid composition.

Chemical diffusion

Dissolved ions move within the fluid according to a process called chemical diffusion. Diffusion occurs due to the random motions, driven by chemical potential, at the atomic scale that leads to a net flux of particles in the fluid (Zhang, 2010).

The diffusion characteristics of dissolved ions depend, among others, fluid temperature, the solvent density, local ion concentration, chemical potential, and molar mass. Laboratory experiments on different fluid matrices estimates the diffusion coefficient of the particles at different temperatures.

Holt & Vasmel (2009) propose a quantitative method to estimate the transport velocity of a dissolved ion in a fault, by diffusion. They simplify flow characteristics within a fault by modelling it as a tube. Thereby, it is possible to estimate the time necessary for certain ions to move from a zone with a higher concentration to a location with a lower concentration.

To model ion diffusion, we use Fourier's Equation 2.1:

$$\frac{D\ t}{d^2} = \frac{C_1 - C_{center}}{C_1 - C_0}$$

Equation 2.1

Where D is the diffusion coefficient, d is the distance between the source location and the location of interest, C_0 is the concentration of the ion at the location of interest at t = 0, C_1 is the concentration at the source location and C_{center} is the concentration at the middle of the tube on the location of interest.

Physical water flow

Mineral dissolved in the water are also transported by the flow of the groundwater *Cunningham & Williams, 1980). Fluid flows only if there are differences in pressure potential, accordingly to Darcy's law (Equation 2.2). The speed of the flow in the subsurface depends on the size of the hydraulic conductivity of the ground (higher if fractured soil) and on the pressure difference.

$$Q = \frac{kA}{\mu L}\Delta P$$

Equation 2.2

Q is the flux (in m^3/h) of the fluid, k is the permeability of the medium, A is the sectional area, μ in the dynamic viscosity, L is the length of fluid's path and ΔP the total pressure difference.

3

Findings

Lithium in the Dutch subsurface can be present for different reasons. The following chapter reports the possible sources of lithium based on literature research and the fields and formations where lithium is found in the Dutch subsurface.

3.1. Literature: sources of lithium

Lithium is mainly mined from igneous rocks (Latunussa et al., 2020). Higher lithium concentrations can also be found in evaporates, such as anhydrite and clays (Bradley et al., 2017). No salt minerals (such as halite minerals) are known to contain lithium, but it was found that the metal present in minerals such as lepidolite, can interact with $MgCl_2$ solutions, leaching in the salt rocks (Mertineit & Schramm, 2019).
The main lithium deposits differ in igneous (pegmatites), sedimentary (clays) and brine (anhydrite). As can be seen in Figure 3.1, the biggest lithium deposit in Europe comes from igneous sources, with some sedimentary sources closer to Turkey. The figure also shows the geothermal source in the Upper Rhine Valley in Germany.
The highest reported concentrations of lithium in Europe are in the area of the Variscan belt, in the south and central Europe (Latunussa et al., 2020). The metal has been extracted from volcanic granitic pegmatites where the most abundant minerals are lithium-rich micas such as lepidolite and petalite. Other minerals were found also in other pegmatite intrusions with high lithium concentrations such as ampblygonite, elbaite, eucryptite montrebasite and jadarite but also deposits of lithium-cesium-tantalum pegmatites such as Wolfsberg were found in Austria (Bradley et al., 2017).

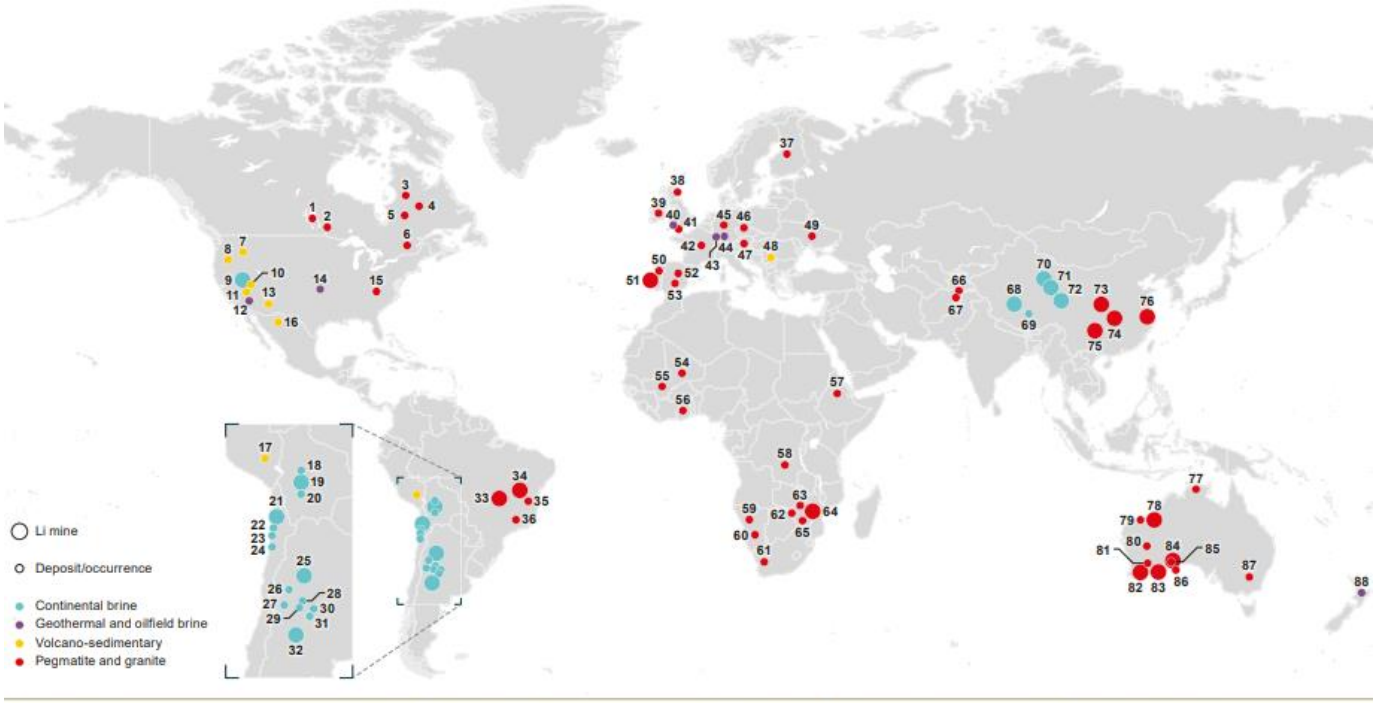

1 Tanco, Canada
2 Separation Rapids, Canada
3 James Bay, Canada
4 Rose, Canada
5 Whabouchi, Canada
6 Val-d'Or, Canada
7 McDermitt, USA
8 Kings Valley, USA
9 Silver Peak, USA
10 Bonnie Claire, USA
11 Boron, USA
12 Salton Sea, USA
13 Clayton North, USA
14 Magnolia, USA
15 Kings Mountain, USA
16 Sonora, Mexico
17 Falchani, Peru
18 Salar de Coipasa, Bolivia
19 Salar de Uyuni, Bolivia
20 Salar de Pastos Grandes, Bolivia
21 Salar de Atacama (2 operators), Chile
22 Salar de Aguilera, Chile
23 Salar de Pedernales, Chile
24 Salar de Maricunga, Chile
25 Salar de Olaroz, Argentina
26 Salar de Cauchari (2 projects), Argentina
27 Salar del Rincón (3 projects), Argentina
28 Salar de Pozuelos, Argentina
29 Salar de Pastos Grandes, Argentina
30 Salar de Ratones, Argentina
31 Salar de Diablillos, Argentina
32 Salar del Hombre Muerto (3 projects), Argentina
33 Mibra, Brazil
34 Mina da Cachoeira, Brazil
35 Jequitinhonha, Brazil
36 Volta Grande, Brazil
37 Länttä (and 5 others), Finland
38 Glenbuchat, United Kingdom
39 Aclare, Ireland
40 United Downs, United Kingdom
41 St Austell, United Kingdom
42 Chédeville (and 4 others), France
43 Rittershoffen, France
44 Upper Rhine Valley, Germany
45 Zinnwald (and 4 others), Germany
46 Cinovec, Czech Republic
47 Wolfsberg, Austria
48 Jadar, Serbia
49 Polokhovskoe (and 2 others), Ukraine
50 Mina do Barroso (and 3 others), Portugal
51 Alijó, Portugal
52 Valdeflórez/San José, Spain
53 Alberta I, Spain
54 Bougouni, Mali
55 Goulamina, Mali
56 Ewoyaa, Ghana
57 Kenticha, Ethiopia
58 Manono-Kitotolo, Democratic Republic of Congo
59 Uis, Namibia
60 Karibib, Namibia
61 Orange River Area, South Africa
62 Kamativi, Zimbabwe
63 Zulu, Zimbabwe
64 Bikita, Zimbabwe
65 Arcadia, Zimbabwe
66 Parun area, Afghanistan
67 Nuristan area, Afghanistan
68 Zhabuye Salt Lake, China
69 Dangxiongcuo, China
70 West Taiji Nai'er, China
71 East Taiji Nai'er, China
72 Qinghai Salt Lake, China
73 Sichuan Aba, China
74 Maerkang, China
75 Jiajika, China
76 Ningdu, China
77 Finniss, Australia
78 Pilgangoora, Australia
79 Wodgina, Australia
80 Kathleen Valley, Australia
81 Mount Holland, Australia
82 Greenbushes, Australia
83 Mount Cattlin, Australia
84 Mount Marion, Australia
85 Bald Hill, Australia
86 Buldania, Australia
87 Narraburra, Australia
88 Ohaaki, New Zealand

Figure 3.1: Lithium deposits distribution around the globe (Shaw, 2021).

Lithium Sources in neighboring countries

Lithium was found in Germany, transported and accumulated in Upper Permian (Zechstein) salt deposits in the Gorleben and Morsleben structures of the northern Germany from other sources (Mertineit, 2019). The Zechstein group from the North German Basin, extends from the North Sea east to Poland shown in Figure 3.2 (Wong et al., 2007).

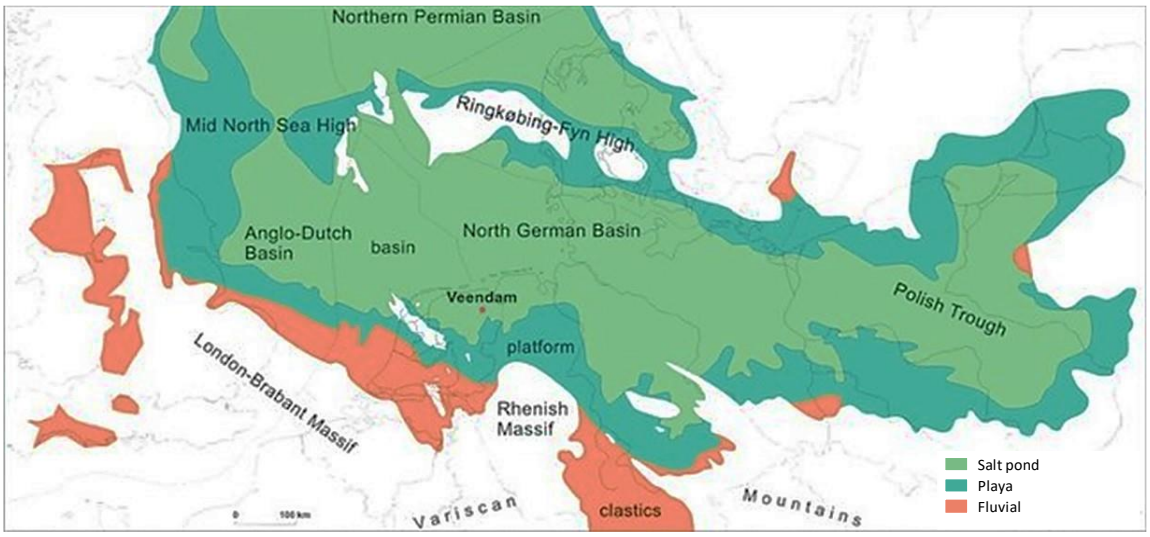

Figure 3.2: The distribution of Zechstein Group at present (Wong et al., 2007).

Lithium concentrations in aquifers of the Zechstein formation were found in the Upper Rhine Graben, making possible to begin the extraction of Lithium from geothermal brines. The metal, dissolved from the Zechstein formation in the geothermal waters, will be extracted in the areas of Insheim and Landau (Wedin, 2022).

3.2. Lithium in the Dutch subsurface

The data of the wells with lithium concentrations publicly available are shown in Figure 3.3. In the figure are plotted the lithium concentrations against their field of origin and reservoir formation.
The lithium concentrations of some fields are publicly available of several wells. The graph in Figure 3.3 shows all the data available of the metal concentrations per well.
Figure 3.3 shows that the highest concentrations of lithium are found in the Zeeland formations and the Upper Rotliegend.
The Upper Rotliegend, in the Akkrum-13 (AKM-13) field, shows the highest lithium concentrations of 47 ppm. The field is an old Chevron field, closed in 1980, but both the data retrieved come from two reports that show similar results, still with 0.7 ppm of variability.

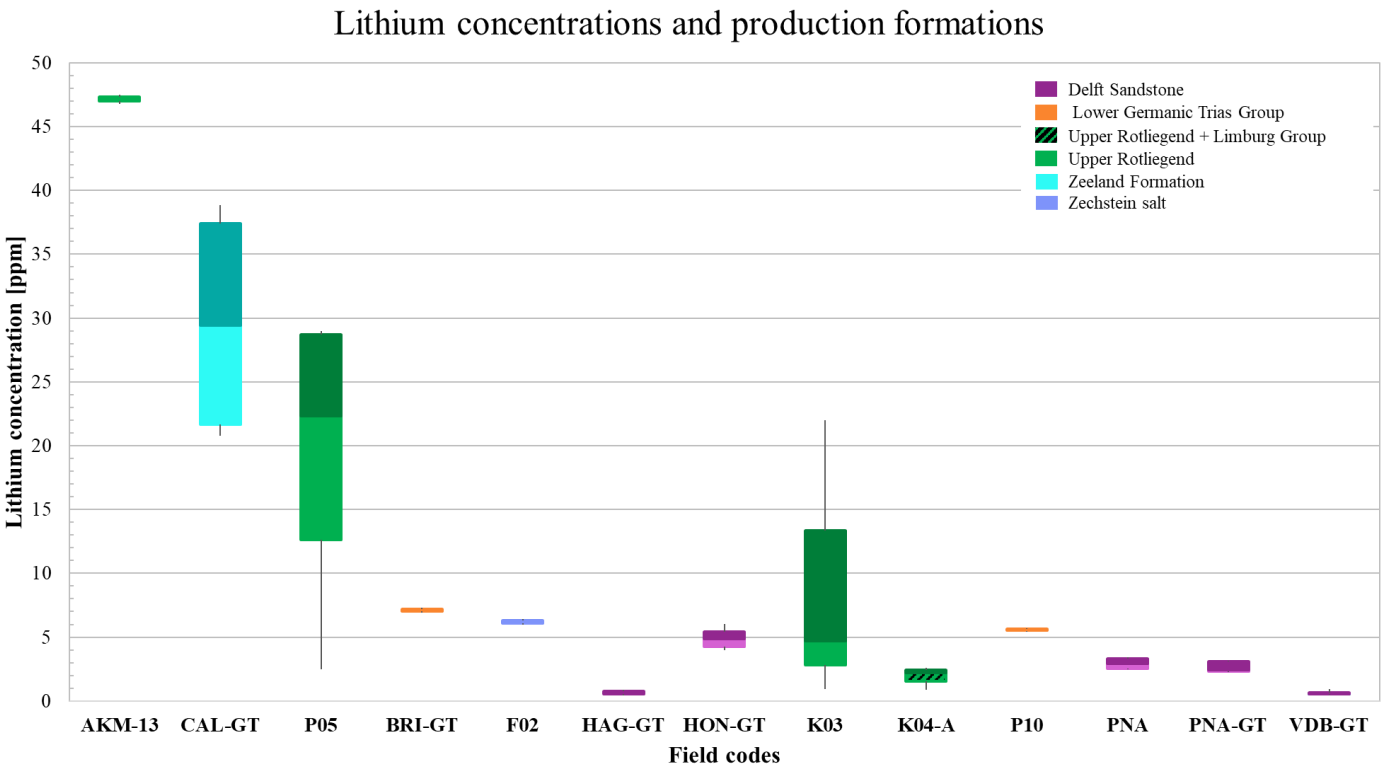

Figure 3.3: Variability of lithium concentrations based on field data results and the reservoir formation.

The other fields producing from the Upper Rotliegend (P05, K03, K04-A) are offshore fields. The variability of the lithium concentration within and between these fields is much higher than the Akkrum-13 gas field. In the P05 field the lithium concentration is in the range between 13 and 29 ppm, whereas in the two K fields the lithium detected was less than 14 ppm.

In only one field producing from the Zeeland Formation the lithium was observed: the Californie Geothermie (CAL-GT), between 20 and 39 ppm. The data come from two different boreholes in the same field but there is no reference on where the sampling occurred.

Two other fields produce from the Lower Germanic Trias Group: the Brielle Geothermie (BRI-GT), 7 ppm, and the offshore P10, 6 ppm, both from a single data point.

The offshore F02 field produces from the Zechstein salt and present lithium concentrations lower than 7 ppm.

Finally, a series of onshore fields produces from the Delft Sandstone: Den Haag Geothermie (HAG-GT), Honselersdijk Geothermie (HON-GT), Pijnaker (PNA), Pijnaker Geothermie (PNA-GT), Vandenbosch Geothermie (VDB-GT).

4

Results

The data retrieved from literature is analyzed and compared with the water compositions from NLOG. The approach used is as it follows: comparison of lithium concentrations with other metals, investigation of lithium concentration in the same formations and an evaluation of the possible sources of lithium based on the areas where it is found based on the geology of the subsurface.

4.1. Mineralogical correlation of lithium with other metals

Lithium has been found in several different minerals as explained in chapter 3.1. As lithium dissolves in the groundwater, also the other minerals present in the rock matrix react with it, resulting in a water with chemical characteristics deriving by different stages of the hydrological cycle (Mercado & Billings, 1975). The scope of this chapter is to analyze if there are any correlations between Li^+ and other metals to eventually predict its presence if some elements are present.

The data obtained from NLOG are used to investigate the correlation between lithium concentration and the concentration of other metals.
The lithium concentration for the field data is plotted against different elements of the minerals containing lithium stated in chapter 3.1.

Lithium in lepidolite minerals

As lithium is found in Europe in lepidolite and petalite minerals, it is of interest to investigate the correlation of lithium ions with other metals commonly present in these minerals. Mertineit & Schramm (2019) made a geochemical analysis of lepidote minerals from the German basin finding that they are composed of 22.74 wt.% Si, 8.38 wt.% K, 14.30 wt.% Al, 2.42 wt.% Li, 1.54 wt.% Rb and 0.32 wt.% Cs. Petalite has the chemical composition of $LiAlSi_4O_{10}$ (Sitando & Crouse, 2012).
As lithium reacts with groundwater, the other elements in the minerals dissolve in the waters enriching their chemical composition. For this reason, the correlations of the Li^+ with these elements are investigated, as shown in Figure 4.1. Cesium (Cs) and rubidium (Rb) are uncommon metals in aquifers (with concentrations lower than 6 µg/l (Mathurin et al., 2014)), but due to their presence in lepidolite, their concentrations are expected to be indicative for the lithium concentration in the water.

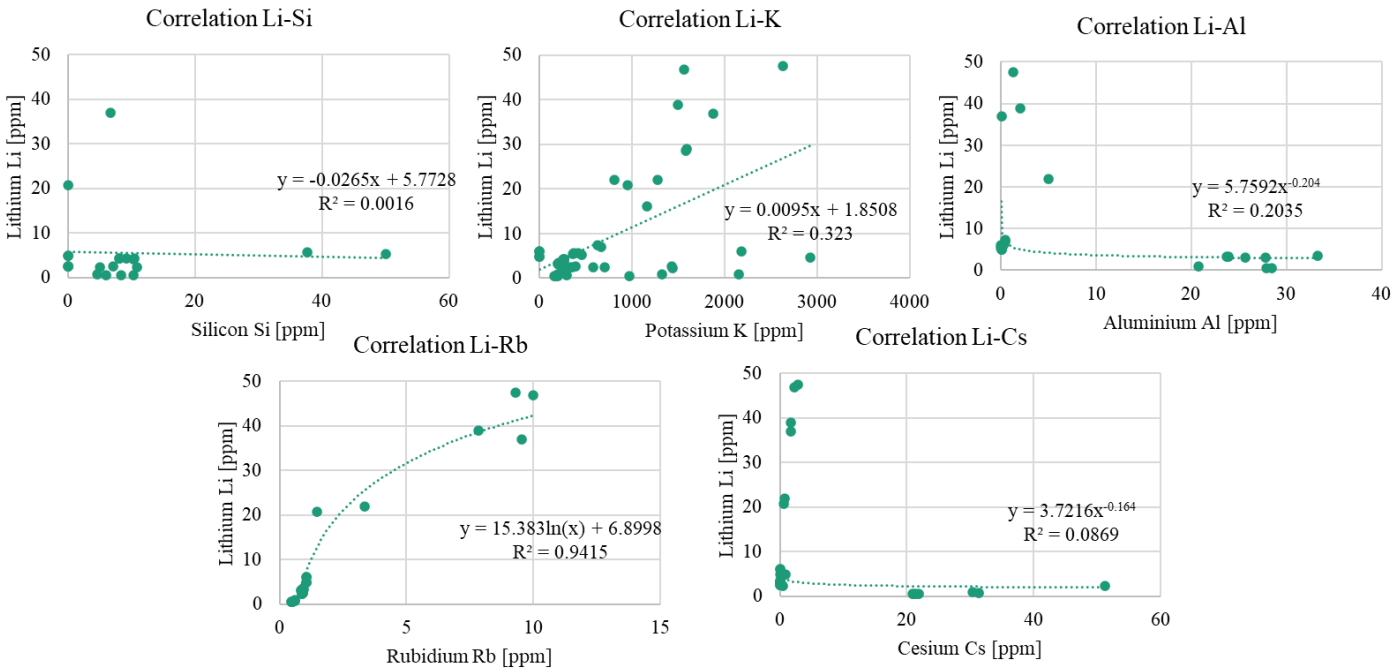

Figure 4.1: From top left to bottom right: Correlation graphs between Li-Si, Li-K, Li-Al, Li-Rb, Li-Cs.

The Li-Si, Li-Al, Li-Cs graphs show that Li concentration is not strongly correlated with the elements, even with the best fit. For low concentrations of K and Rb it seems that also Li has low values. However, the Li-K does not show a correlated with K concentrations >700 ppm, in which case the Li is in the range of 0 to 46 ppm; higher concentrations of K does not always correspond to higher Li concentration. Concerning Li-Rb correlation: there a strong correlation between the metals, indicated with the R^2 value of 0.94. However, there were only 13 samples with both elements analyzed, too few to draw a strong conclusion.

$MgCl_2$ and lithium

As stated from the paper of Mertineit & Schramm (2019) and explained in chapter 3.1, lithium can migrate through the subsurface due to chemical reactions with $MgCl_2$. It is to expect a correlation between lithium and Mg^{2+} and Cl^- ions. However, because magnesium and chlorite concentrations are usually far greater than lithium concentrations, we do not expect a strong relationship between these metals.

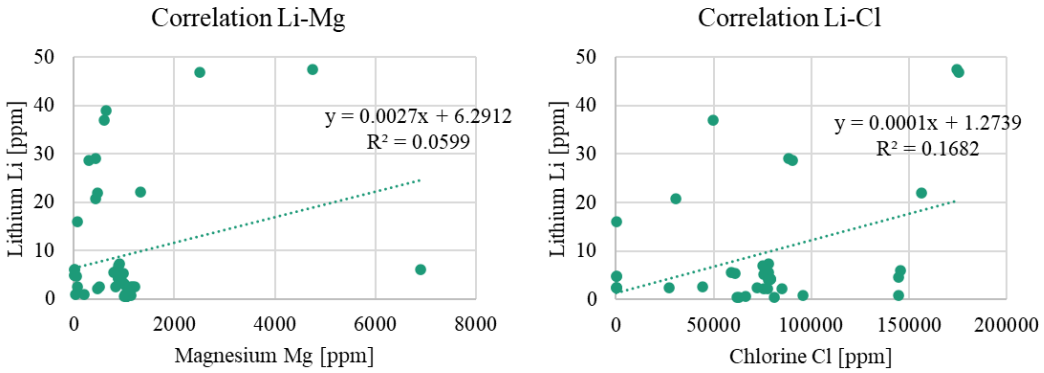

Figure 4.2: On the left graph showing the concentration of Li compared to Mg and on the right Li-Cl graph.

Figure 4.2 show that also in these cases there is no strong correlation between the Mg^{2+}, Cl^- and the Li^+ concentrations in the aquifers, with R^2 values lower than 2. Most of the samples show magnesium concentrations lower than 2000 ppm, but the concentrations of lithium vary without a trend relative to the concentration of the other element. Similarly, the chlorine concentrations do not show a strong correlation with the lithium concentrations.

Lithium and other metals

The analyses of the correlation of lithium concentration with other metals (Na, Cu, Sr, Mn, Ca, Pb, Fe, F, Cd, Ni, P, B, Zn) are presented in Appendix A. These analyses show there is no strong correlation with these metals.
There is no element besides Rb found in the water analyses of the Dutch subsurface that is strongly correlated the lithium concentration. The correlation with Rb is based only on 13 samples. This indicates that it is not possible to estimate the lithium concentration in an aquifer using the concentration of another metal.

4.2. Presence of lithium in specific formations

In chapter 3.2 the concentrations of lithium in different the formations are shown.
The location of the wells from which the lithium concentration is known are presented in Figure 4.3 (for more detailed information about the field shape and the exact well coordinates refer to the NLOG webpage).

Concentrations and formations

The concentrations of the metal vary significantly between different fields producing from the same formations. Data of the Upper Rotliegend reservoir fields show a concentration rang of 47.5 to 0.95 ppm, with significant variations even withing the same field, see Figure 4.3. The lithium concentrations vary of more than 40 ppm for the 4 fields, indicating that the formation is not necessarily an indication of high lithium concentrations.
The metal was identified in only one field producing from the Zeeland Formation and the Zechstein Salt, thus not sufficient to conclude any typical lithium concentrations for these formations.
The two fields of the lower Germanic Trias Group, one onshore and one offshore, show similar low lithium concentrations, but it is again improper to make assumptions of the characteristics of the whole formation based on two wells.
The highest amount of data came from wells with Delft Sandstone as reservoir rock. The samples, coming from 5 different fields all show low lithium concentrations, ranging between 0 and 5 ppm.

Formations locations

The fields with formations from the Upper Rotliegend are located both offshore and onshore, so there is high lateral and longitude variability. The difference in lithium concentration between different fields suggests that the lithium concentration in the Upper Rotliegend is not related to the depositional settings of a single formation in the Netherlands, but due to other factors. The difference in lithium concentration within a single field (P05-01) can be a consequence of different analysis and sampling methodologies applied to determine the lithium concentrations (unfortunately not all present on NLOG) or differences in water-rock interaction due sedimentary heterogeneity on a field-scale (MacEachern, 1992). The variation of the field-averaged lithium concentrations (9-48 ppm) within a

single formation suggests that lithium in the Upper Rotliegend is not present due to the depositional history and depositional environment.
The lithium concentration in the Delft sandstone is consistently in the range of 0.5-6 ppm for all the fields considered, however, due to their proximity (maximum 45 km distance) no meaningful lateral-extrapolation of the lithium concentration within this formation can be made.

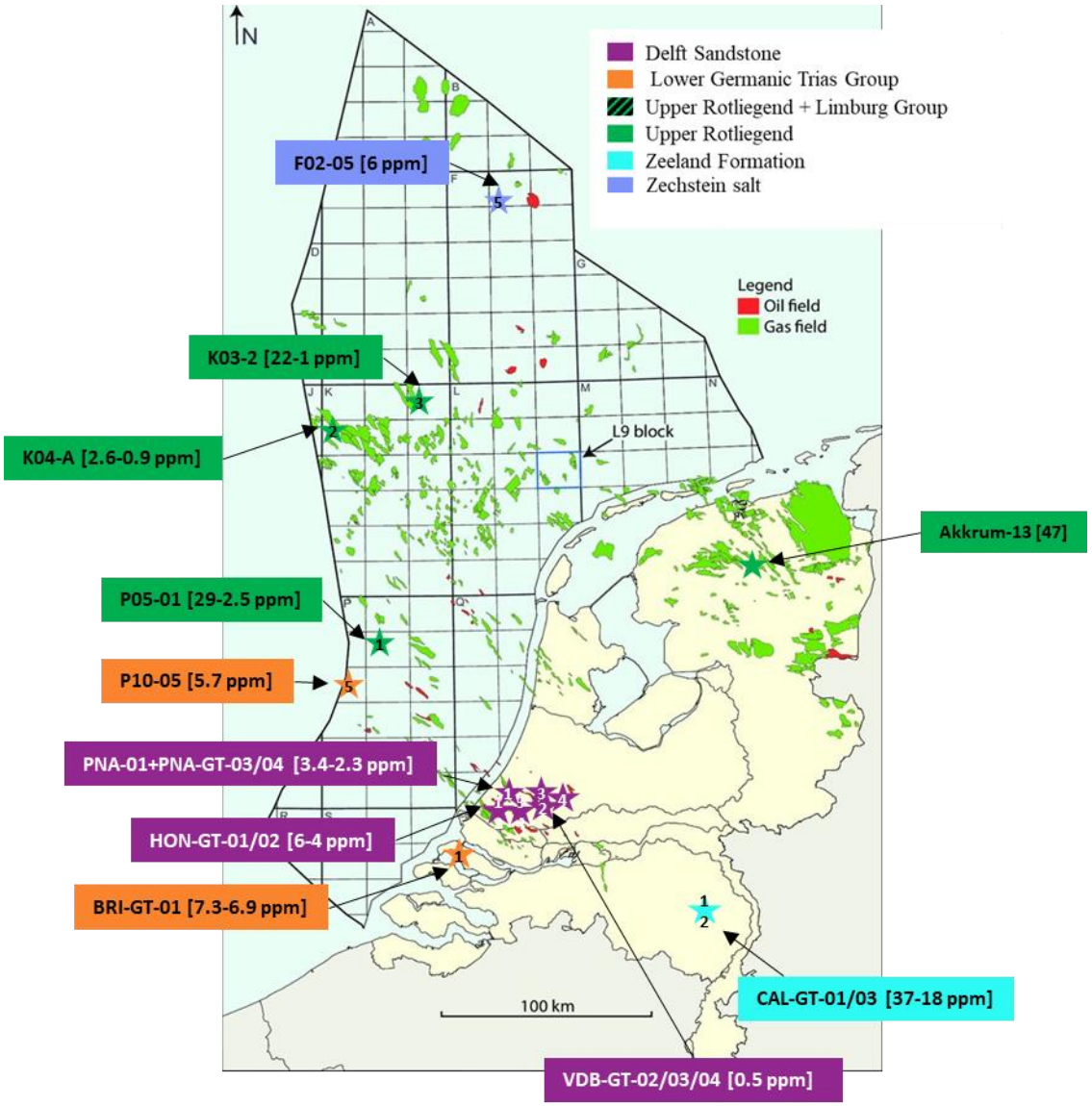

Figure 4.3: Locations at the surface of the borehole wells with indicated the range of lithium concentration found and the production formation. (Locations retrieved from NLOG and map from Jager (2012)).

4.3. Lithium sources based on the geology of the subsurface

Neither the presence of different elements or the era of depositional environment (formation) are indicators or explain the presence of lithium.
The main source of the metal in Europe are intrusive rocks, as explained in chapter 3.1. Since two major volcanism events involved the geology of the Netherlands, this subchapter examinates if there are any relations between these and the lithium found in the Dutch subsurface.

4.3.1. Geology of the subsurface and lithium concentration

The Dutch subsurface has gone through several phases of rifting and tectonic stresses that induced the opening and reactivation of a several sets of major faults (Wong et al., 2007).

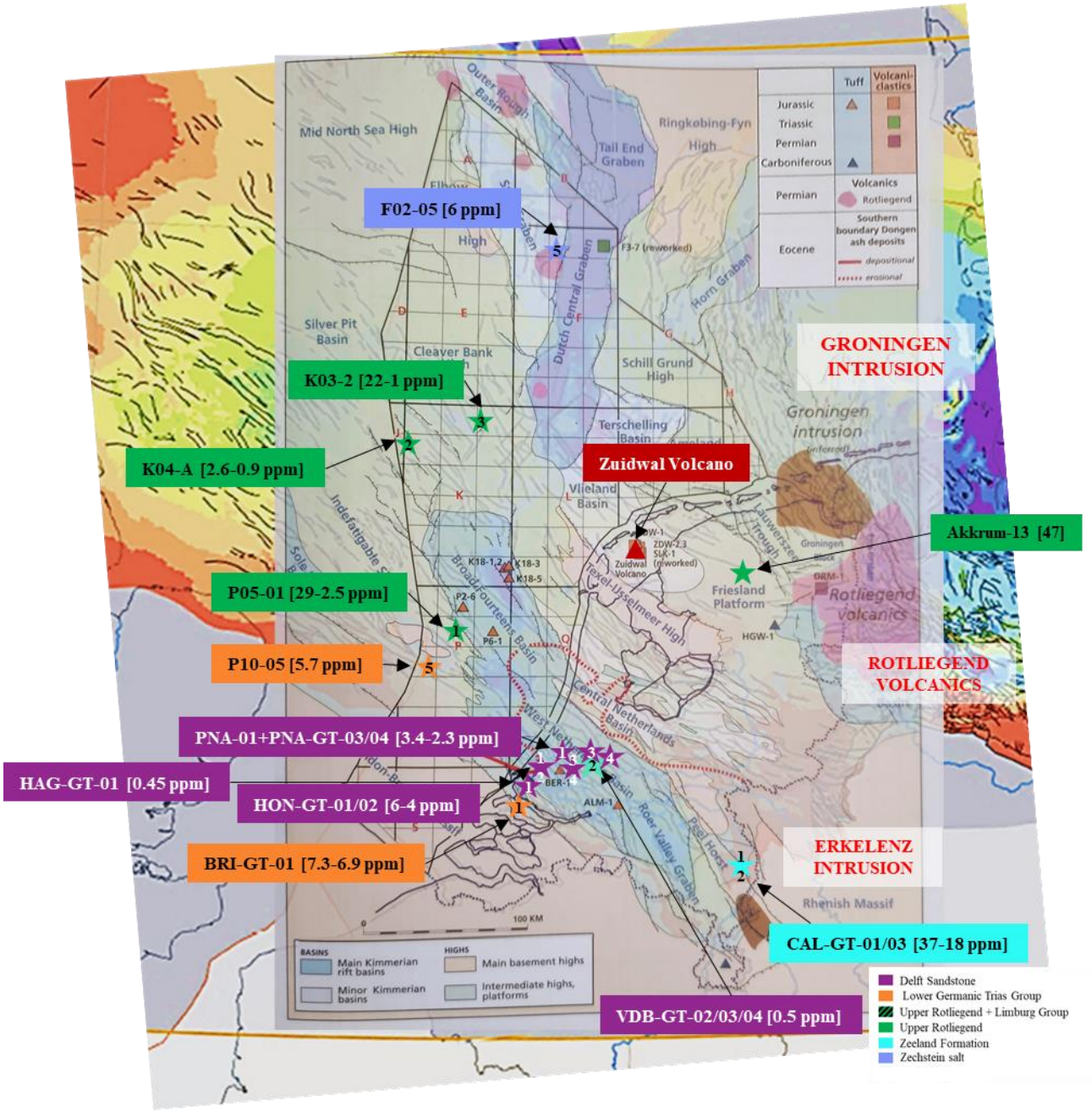

Figure 4.4: Well locations on map showing the major fault systems running through the Dutch subsurface (Doornenbal & Stevenson, 2010) together with the main intrusions due to the 2 major volcanic events in the Netherlands (Wong et al., 2007).

The Permian igneous rocks (Rotliegend) are from the same tectonic even that caused volcanic intrusion in the northern part of Germany in the Ems Graben and Poland. In Figure 4.4 are shown the location of the wells on a map that combines the major volcanic intrusions (from the map of Figure 2.2). From the figure it is evident the large quantity of faults running from the intrusion through the land, where the Akkrum-13field is.

It is possible that the lithium present in the Akkrum-13 field has been transported by the water flowing in the formation, from the volcanic region to the reservoir of the same formation, facilitated by the fractures in the subsurface. But to further investigate this, more aquifer samples of the area closer to

the intrusions are necessary. From the cross section of the area crossing the Akkrum-13 field in Figure 4.5, on top of the thin reservoir layer there is a thicker Zechstein formation. The Rotliegend runs from the left most part of the cross section until the Friesland Platform where it was eroded. The mineral dissolution and transportation are then not to be expected further that the Friesland Platform.

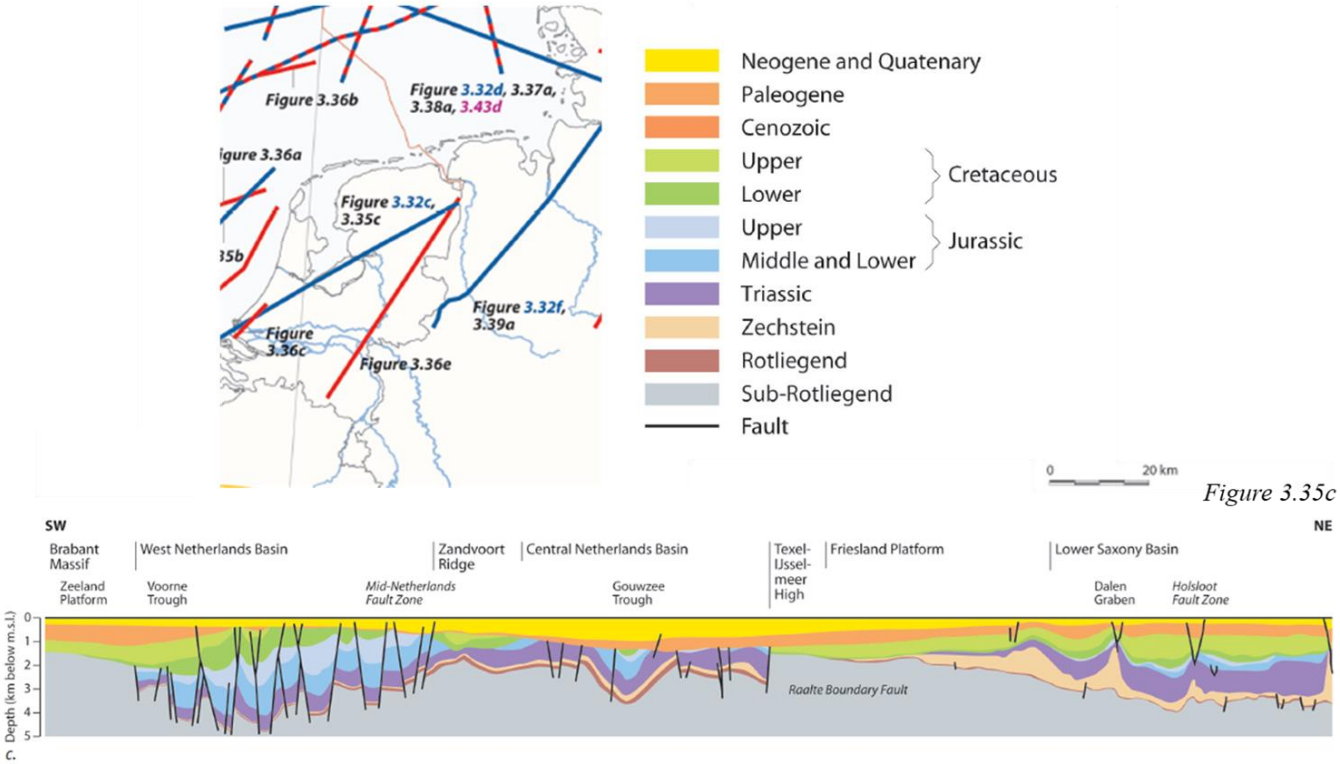

Figure 4.5: Cross section of the Netherlands from SW to NE (Doornenbal & Stevenson, 2010).. The Akkrum-13 field is located on the left side of the Lower Saxony Basin.

Similarly to the Akkrum-13 gas-field, the other field resulting in higher lithium concentration is in a fault zone close to the Erkelenz intrusion at the German border. The Californie geothermal field is located on the major fault system passing through the Peel Horst, connecting the intrusion to the field. Some other small Rotliegand intrusions appear also in the upper most part of the Dutch off-shore, from which only one well, the F02-05, show some lithium concentrations, as well as the K03 field. This well, is the only well that produces from the Zechstein salt deposited right after the Upper Rotliegend. If in the previous chapter 3.1 is stated the mobilization of lithium ions due to the salt minerals, the salt deposited on above the igneous rock, the lithium present has then not been transported by the salt.

Besides these two major intrusions, the map shows the Groningen intrusion. Unfortunately, there are no data available indicating the metal composition of the subsurface in the Groningen field, so it is impossible to know if the area has higher lithium values related to the nearness to the intrusions and the high series of faults.

The cross section in Figure 4.6 shows that the Permian layers in the NNE part of the section are eroded and Cretaceous rocks are in contact with the Upper Carboniferous. If the lithium present in the subsurface is from the Rotliegend volcanic events, in the Californie Geothermie region it must have travelled from a further source since the Permian rocks have been eroded and the Triassic lays on top of the Upper Carboniferous.

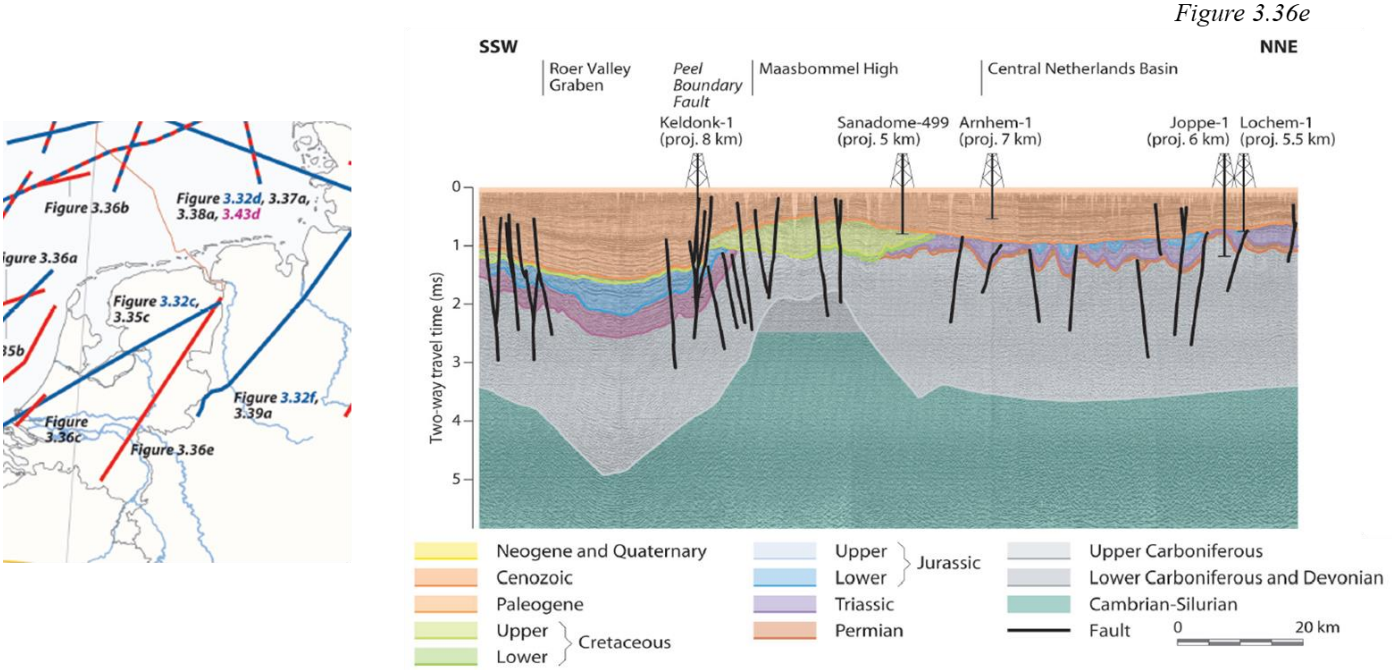

Figure 4.6: Cross section of the Dutch German border. Permian rocks (as the Upper Rotliegend) appear onlyi in the most right side of the cross section, cutted by the Cretaceous formation further on the left (Doornenbal & Stevenson, 2010).

4.3.2. Theoretical exercise of lithium transport from water along faults

As explained in chapter 2.3, lithium could have also been transported in the subsurface because of chemical diffusion in the groundwater and the physical flow of water along the faults.

Chemical diffusion

From the method proposed by Holt & Vasmel (2009) to estimate the dissolution time of a molecule in water, it is possible to estimate the time necessary for lithium to move from a highly concentrated zone, where the metal dissolves in water from the source rock (igneous rock), to a further location. The distribution of diffusion coefficients of lithium ions in water at different temperatures can be seen in Figure 4.7 (Fan et al., 2016).

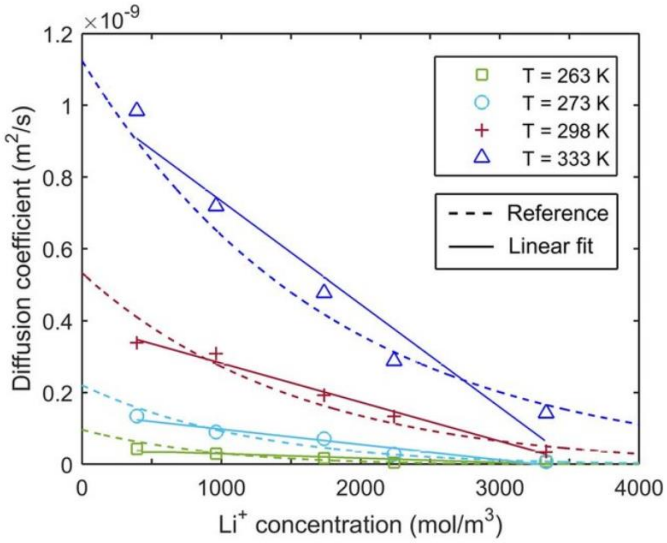

Figure 4.7: Diffusion coefficient of Li+ in water as function of concentration at different temperatures (Fan et al.,2016).

Given the Fourier's diffusion equation (Equation 2.1), the diffusion coefficient of dissolved lithium is considered at T = 335 K, circa 600 m in depth, and taking into account an initial C_0 = 300 ppm (so 43 mol/m^3), based on the high brine concentrations in the near Upper Rhine Valley (Wedin, 2022) of > 200 ppm. It is considered C_1 = 43 ppm, C_{center} = 47 ppm as the concentration in the Akkrum-13 field, d = 50 km, and D = $1x10^{-9}$ m^2/s. The time for lithium ions to move at this distance would be of 4e+16 s so more than 1200 Ma.
If this model would represent the real only movement of lithium ions in the subsurface, the ions would take ¼ of the Earth's lifetime to move of 50 km in the subsurface and the lithium would be present only in the proximity of the source mineral.

Physical water flow

In this second model it is assumed that the lithium is homogenously transported by the normal groundwater flow in the subsurface. Along faults water velocities range from 13 up to 242 m/d (Medici, West & Banwart, 2019). Groundwater flow reaches the highest speeds closer to the surface, where the hydraulic conductivity is higher.
Considering the slowest flow rates, to travel along a set of faults 50 km long perfectly connected the water takes less than 77 years.
A similar investigation was done by Lapperre et al. (2019) where the groundwater level of the Roer Valley Rift System, a highly faulted zone in the southern part of the Netherlands close to the Eifel volcanism, is investigated. The paper points out that the permeability of the area is reduced blocking the groundwater flow in some areas.
Other sources state that the groundwater flow in aquifers is considered fast when it is around 0.3 m/d and can be as slow as 0.3 m/y (Alley et al., 2013). Considering the fastest case, due to the fractures in the faults, the water would take 42 days to flow for 50 km in the subsurface.
Finally, considering the flow rate of 0.3 m/y, the water takes 15000 years to flow 50 km.
At this last flow rate, the metal dissolved in water can move from the source rock until 400 km away, as the distance from the Akkrum-13 field to Insheim in less than 0.2 Ma.
From this last result, it is reasonable that the fields with Upper Rotliegend formations as reservoir rock contain lithium concentrations probably coming from the closest Rotliegend volcanism intrusion. 0.2 Ma for mineral migration is in fact much lower that the time to success to a different formation (after 5 Ma circa from the Upper Rotliegend the Zechstein salt started its deposition (NLOG)). Hence, it is likely that the lithium comes from the closest volcanic intrusion, occurred in the same age and/or transported by the water along the highly faulted areas.

5

Geothermal brine mining

Of the methods already used to extract lithium, the extraction of the metal from salar brines is of more interest for this research than the techniques used to separate it from the mined pegmatitic rock. This chapter is focused on the methodologies for lithium extraction from brines and on the variations necessary for a geothermal plant to extract the metal.

5.1. Methodologies of lithium extraction from brines

The extraction of lithium from brines currently in operation has as intermediate products LiCl (lithium chloride) and Li2CO3 (lithium carbonate), usually refined to LiOH·H2O (lithium hydroxide) for commercial use.

Technologies for direct lithium extraction (DLE) include reverse osmosis (RO) and nanofiltration (NF) membranes, adsorbent materials such as ion exchange and sorbents, and electrodialysis processes. This section focuses on similar aspects of these four technologies, such as lithium's selectivity and recovery *R* from competing ions, the resilience of the material to solids, water composition stream temperature, and flow speed. Comparing the same aspects of DLE is important in the context of developing future projects on lithium extraction from geothermal brines. Commercially available and developed methods are more likely to be adapted to geothermal applications. The surface area necessary to operate the technology determines the project's economics, including the materials needed to treat the waters and the nature of the downstream fluid.

In filtration processes, the permeate or filtrate is the filtered stream leavening a membrane filtration system. The name of the material adsorbed by the membrane is retentate or concentrate, as seen in Figure 5.1. The recovery (*R*) is the ratio of recuperated lithium mass over the feed mass of lithium. The rejection coefficient (or retention rate) (*r*) is the difference is defined as follows in Equation 5.1:

$$r = \frac{C_f - C_p}{C_f} \times 100\%$$

Equation 5.1

wherein C_f is the feed concentration and C_p is the concentration of the permeate (Sun et al., 2015 and Li et al., 2019). A negative rejection coefficient means that the concentration in the filtrate of a specific ion is higher than in the feed solution.

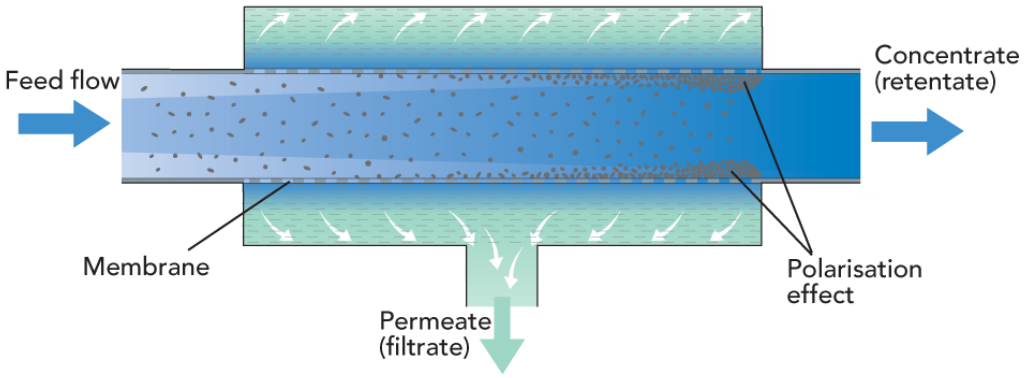

Figure 5.1: Schematic representation of cross-flow filtration with membrane (Bylund & Tetra Pak Processing Systems AB, 2015). The untreated fluid (feed) flows through the compartment. A membrane layer, usually with specific pore size, is situated around the feed's stream. Two streams discharge a filtration system, the permeate and the concentrate. If the pressure difference across the membrane is sufficient, particles smaller than the membrane's pores cross-flow the layer in a stream called the permeate or filtrate. Concentrate is the fluid or solid with the unfiltered materials, adsorbed in the membranes or still dissolved in the fluid. The polarization effect blocks the transport of material. A screen of polarized ions concentrates at surface or pores of the membrane due to the selective transport through the filtration layer.

5.1.1. Extraction of lithium from mining brines

Methodology

In the mining industry, the metal is extracted from the brines through a series of evaporation processes in evaporation ponds. The water in the brine after months evaporates from the pond until the metal remains in high concentrations of crystals. The other elements in the brine precipitate progressively in the series of ponds until an optimal lithium concentration is reached.

Selectivity and Disadvantages

The lithium concentration factor (CF) is 1.06; the brine concentration can reach values up to 2120 ppm after this process. The brine is usually further refined to obtain a product with fewer impurities.

This method can take months to years depending on the weather and climate and requires a sizeable superficial area exposed to the sun. In addition, most of the extracted material is not economically valuable and must be disposed of or stored for later processing (Stringfellow & Dobson, 2021a).

5.1.2. Membranes

Membranes are physical barriers that separate two phases and selectively restrict the transport of various chemical compounds. The separation occurs via size exclusion, charge, and stability reactions (Zhang et al., 2020). Several membrane techniques have recently been reviewed and described by Stringfellow & Dobson (2021a). The paper evaluates various membrane extractions and the different patented solvents used for lithium absorption. A large scale of lithium-selective membranes has been tested on the laboratory scale to directly extract the lithium. Nanofiltration and Reverse Osmosis membranes can be prospective for future lithium extraction. Figure 5.2 illustrates a schematic representation of the principles of membrane filtration.

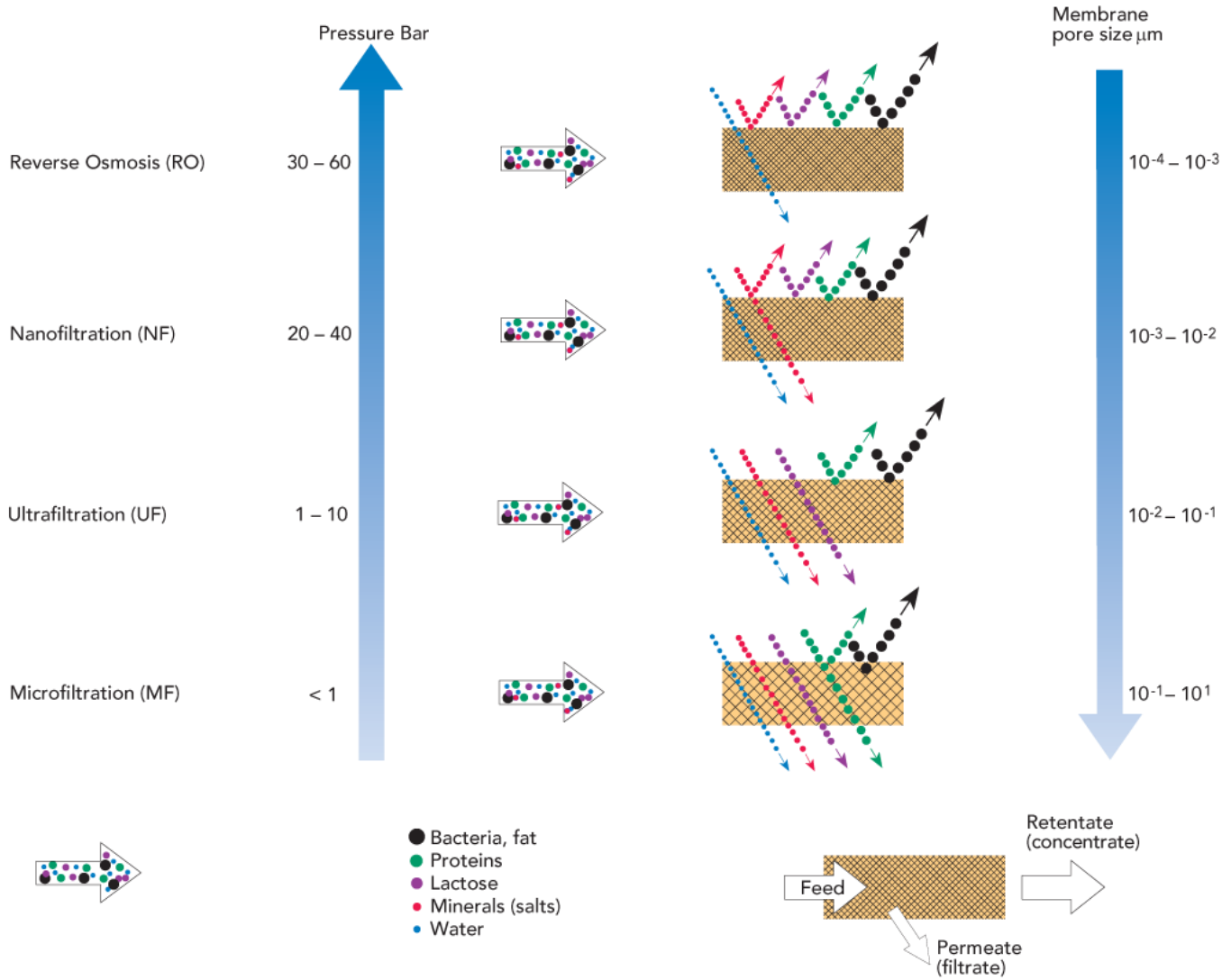

Figure 5.2: Principles of membrane filtration (Bylund & Tetra Pak Processing Systems AB, 2015). The pore sizes determine the name and operational pressure for membrane filtration. RO membranes have the smallest pore size of 10^{-4}-10^{-3}µm (right arrow), operating at the highest pressure of 30-60 bar (left arrow). The membrane has also the highest rejection; the retentate contains all materials dissolved in the feed and only water molecules permeate the filter (drawing between the arrows). From NF to MF the pores are wider (from 10^{-2} to 10^{1} µm) and operates at lower pressure (from 20 to <1 bar). The membranes block less material, the permeate in NF contains water and salts, in UF the filtrate has also lactose and in MF only bacteria and fat remains in the concentrate.

Reverse Osmosis Membranes (RO)

Reverse osmosis is the process of forcing pure water molecules through a semipermeable membrane (with pores <0.002 µm) that allows the passage of water but no other materials (Manahan, 1994 and Wagner, 2001).

Selectivity and Recovery:

The membrane's selectivity is affected by the presence of other ions, and it is not selective for only lithium (Somrai et al., 2013 and Stringfellow & Dobson, 2020b). Stringfellow & Dobson (2020b) suggest that the method can only be used as a pre-treatment to concentrate the brine composition. Somrai et al. (2013) investigate the efficiency of separating lithium from Na^+ ions given a specific Mg^{2+}/Li^+ mass ratio of 60, with a concentration of 59.9 ppm lithium ions. The method used in the paper shows that the sodium and lithium rejection rate ranges between 70% and 90%, without a difference in selectivity. Hence, both ions have highly reduced concentration in the retentate. RO membranes, according to other research (Swain, 2017 and Porter, 1990), have lithium recovery up to

99.6%. However, they also reject other ions with recovery higher than 96%, such as calcium, sodium, and potassium, as shown in Figure 5.3.

Ion	Ionic Radius Coordination(6), Å	Feed, mg L^{-1}	Permeates, mg L^{-1}	Rejection efficiency (%)
Calcium	1.00	65	0.2	99.6
Sodium	1.02	150	3.0	98.0
Pottasium	1.38	12	0.3	97.4
Lithium	0.74	0.17	0.0006	99.6
Bicarbonate		19	0.7	96.2
Sulfate		189	0.4	99.8
Chloride		162	2.9	98.2
Nitrate		97	3.5	96.4
TDS		693	11.0	98.4

Figure 5.3:Rejection efficiency of different ions in the reverse osmosis process (Porter, 1990).

Resilience of Material:

Resilience to solids in water

Solid particles such as sand can damage the membrane. The particles can break the filtering film and create holes in the membrane at high flow speed. When the membrane is damaged it is possible only to replace the membrane (Porter, 1990).

A filter with 10 to 20 µm pores must purify the feed from solid particles before entering the reverse osmosis system (Wagner, 2001). In geothermal plants, to protect the injection well, a filter eliminates particles with sizes bigger than 10 µm (DutchFiltration, 2018). Thus, it is not necessary to add a pre-treatment to the feed in a geothermal system.

Resilience to water composition

The membrane is highly affected by strongly acidic or basic solution, as well as strong oxidizing agents and solvents that can dissolve the membrane (Wang et al., 2004).

Resilience to temperature fluctuations

The membrane is sensitive to temperature fluctuations and generally it cannot operate at temperatures higher than 45 °C for RO (spiral wound). At lower temperatures the flux of feed solution decreases and at higher temperatures the rate of membrane hydrolysis increases, decreasing the lifestyle of the membrane (Wang et al., 2004). The resistance to temperature fluctuations and to the maximum temperature depend, however, on the manufacturing process of the membrane itself.

At constant temperature of 22 °C, the recovery of lithium at the maximum pressure was of 90% (Somrani et al., 2013).

Resilience to flow speed

The handbook of Porter (1990), gives a general description of the effects of flow speed on a RO membrane. The flow speed can also cause damages at the surface of the membrane, decreasing its

efficiency. Enough ΔP is still necessary across the membrane to guarantee the reverse osmosis. As stated in the paper: "As a rule of thumb, each 100 mg/l of dissolved solids is roughly equivalent to one psi of osmotic pressure." Considering that the average concentration of dissolved solids in Dutch aquifers is 879300 ppm (see Appendix A**)**, the feed needs at least 60 MPa of ΔP to operate. Depending on the indications of the membrane manufacturer, the Spiral Wound RO membranes in Figure 5.4 can have different flow rate capacities. Membranes available in commerce can operate at 40 m^3/h (Culligan ®, 2016).

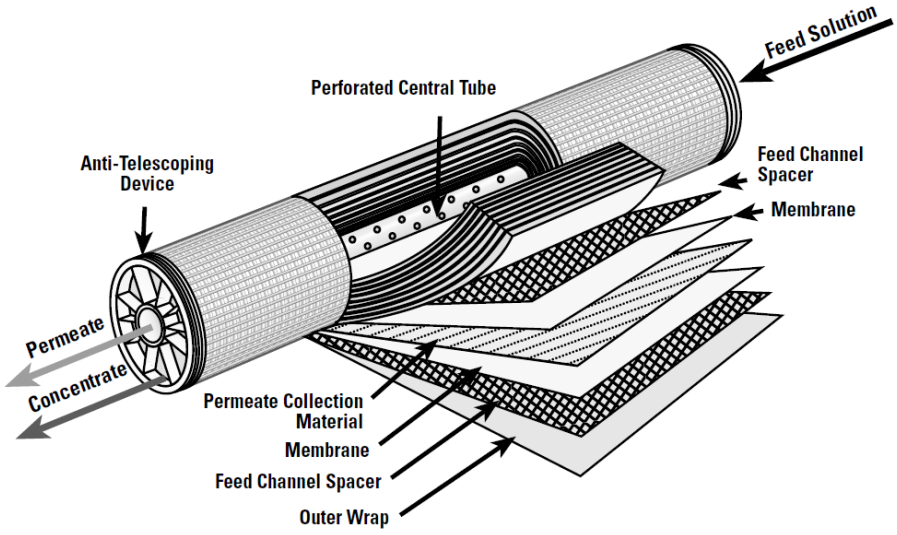

Figure 5.4: Spiral wound RO membrane module (Wagner, 2001). The feed solution enters in the central tube where a series of membranes adsorbs the material that concentrates in the feed channel spacer. The outer trap isolates the tube from air. The anti-telescoping device is located at the end of the membrane to guarantee structural support. The permeate and the concentrate flow from the same direction as the feed solution but in two separated streams.

Ease of sourcing:

RO membranes are already widely used as desalination techniques, in the food and bioproduct industries since they are sensitive to temperature and solvents. They are also used to treat wastewaters in other industrial processes (Porter et al., 1990 and Wagner, 2001).

Space:

RO membranes can be packed from a membrane size of 8.5 m^3 to 0.03 m^3 and they are usually installed in cylinders with diameter of 0.20 m and length of 1.5 m at the maximum flow rate (Porter, 1990).

The RO membrane offered by Applied Membrane Inc. (2020) has a volume of 3 m^3 and can operate at a maximum flow rate of 2 m^3/h. Considering that the maximum flow rate in geothermal projects of 300 m^3/h, if there is a linear relationship between the flow rate and area, the total volume of membranes needed is at least 450 m^3. Generally, the higher the flow rate, the higher the area needed for the membrane facility.

Upstream / Downstream:

Materials necessary

Depending on the membrane used, the manufacturers might require an additional pre-treatment of the brine in addition to the sand filtration (Porter, 1990). Backwash of a chemical solution is necessary

after the filtration to remove the permeate material from the membrane (Porter, 1990, Wagner, 2001, Wang et al., 2004 and Bylund & Tetra Pak Processing Systems AB, 2015).

Impact of wastewater on reservoir

Since the membrane filtration has the same separation efficiency for both sodium chloride ions and lithium ions, the wastewater is removed from most of the salts dissolved (Wagner, 2001, Wang et al., 2004 and Porter, 1990). Due to the lowered salinity of the outlet water, it may need to be replenished with salts to prevent clay swelling if reinjected into the reservoir (Schlumerger, 2022).

Ceramic Membranes/ Nanofiltration (NF) Membranes

Like RO membranes, NF membranes separates fluids or ions from a feed. NF operates like RO filters but the membrane has wider pores, as shown in Figure 5.2. The filtration rejects divalent charged ions and only partially mono-charged cations (Wang et al., 2004, Wagner, 2001). Zhang et al. (2020) Investigates in the detail the separation of lithium ions from other ions with NF membranes.

Selectivity and Recovery:

NF membranes have higher selectivity compared to RO membranes. Several researchers (Somrani et al., 2013, Li et al., 2019 and Gao et al., 2020) report that the retention of divalent ions is higher than monovalent ions. The concentrate has a retention ratio of Ca^{2+} and Mg^{2+} ions of 85%, with lithium and sodium retention rates of around 40% (Li et al., 2019 and Gao et al., 2020). The filtrate contains 60% of the initial lithium under the conditions operated by the research.
Another research (see Zhang et al., 2020) reports that different NF membranes reject 96% of di-charged ions and have lithium retention of only 16%. Hence, 84% of the initial lithium permeates in the filtrate.

Resilience of Material:

Resilience to solids in water

Like the RO filtration method, the NF is sensitive to solid particles and the water needs to flow through filters with pores smaller than 20 µm (Wagner, 2001).

Resilience to water composition

The ion rejection (R) of the membrane is different per ion. Rejection is higher for divalent cations and lower for monovalent cations as following: $R(Mg^{2+}) > R(Ca^{2+}) \approx R(Na^{+}) > R(Li^{+})$ (see also Figure 5.5). The membrane can separate monovalent cations from the retentate. However, the separation of Li^{+} from Na^{+} is inefficient when the sodium concentration is much larger than lithium (in the Dutch geothermal brines is of a factor of 100 larger, as can be seen in Appendix A. Brines have been tested selectively on different NF membranes, and the results show that Li^{+} can reach a rejection rate of ~80%, whereas the ratio C_p/C_f of Mg^{2+} ions is 0.6 (from 40% rejection and Equation 5.1). Na^{+} ions have same rejection as lithium ions of 15%, so filtering does not separate the sodium ions from the permeate (Zhang et al., 2020 and Sun et al., 2015). In addition, the concentration of monovalent ions in the filtrate in NF membranes depends on the feed concentration. The higher the concentration, the more ions are rejected by the membrane (Wagner, 2001 and Somrani et al., 2013).

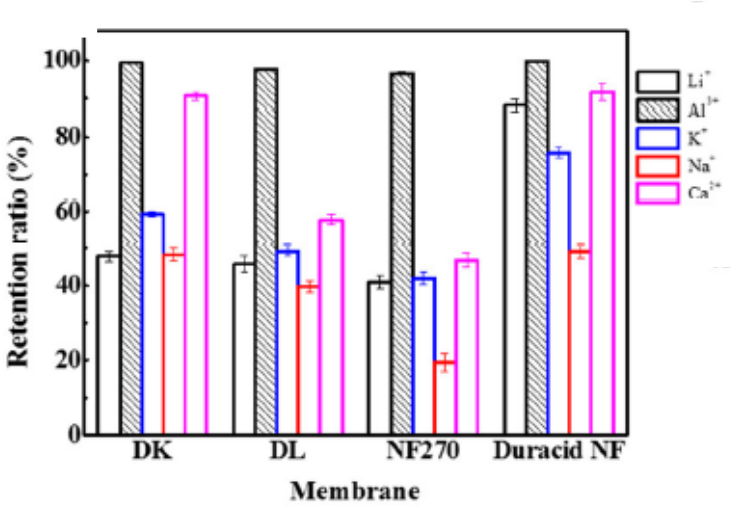

Figure 5.5: Retention ratio of Li^+, Al^{3+}, K^+, Na^+ and Ca^{2+} tested in four NF membranes (Gao et al., 2020).

Resilience to temperature fluctuations

The resilience of the NF membranes depends on their manufacturing process. The operational ranges can be between 9.85 and 49.85 °C (Li et al., 2019).

Sun et al. (2015) tested a NF membrane for separation of Li^+ from Mg^{2+} at different temperatures (25 °C, 30 °C and 35 °C) and observed at the highest ΔP of 2 MPa a rejection of magnesium ions of ~85% at any of the temperatures tested. The lithium retention ratio is lower at lower temperatures.

Resilience to flow speed

The increase in flow rate lowers the rejection of magnesium and lithium ions. As a result, there is an increase in the concentration of magnesium and lithium ions in the permeate (Sun et al., 2015 and Li et al., 2019). Some commercially available NF membranes can operate at maximum flow rate of 1.96 m^3/h (Applied Membranes Inc., 2020)

Ease of sourcing:

NF is used to produce cheaper drinking water (than drinking water obtained with RO) and to reduce the hardness of water due to the high rejection of divalent cations. It is also the membrane technology with the most widespread use in lithium extraction at laboratory-scale (Wang et al., 2004 and Zhang et al., 2020).

Space:

Commercially available membranes operating at 1.96 m^3/h have a diameter of 0.20 m and length of 1 m, with 37 m^3 of active membrane area (Applied Membranes Inc., 2020). At maximum flow rate production of 300 m^3/h, at least 462 m^3 of NF tube membranes would be necessary.

Upstream / Downstream:

Pre-treatment processes are also needed for NF membranes to remove solid particles and ionize the feed. They are well known and specified by the manufacturer of the membrane.

The outlet water flowing from the tube has sodium and chlorine ions 15% lower than the initial concentration. However, lithium is still dissolved in the waters and needs different processes to be separated.

5.1.3. Ion Exchange

Methodology

Ion exchange is used to remove ions from waters. The water flows through a solid anion or cation exchanger where the ions in the water are replaced with the ones at the surface of the exchanger (Manahan, 1994).

Lithium separation is done in a vessel with a cation exchange material. The reactions in the vessel are as shown in Equation 5.2 where {Cat(s)} is the solid cation exchanger

$$H\{Cat(s)\} + Li^+ + X^- \rightarrow Li\{Cat(s)\} + H^+ + X^-.$$

Equation 5.2

A strong acid solution must flow through the vessel to extract the lithium and regenerate the adsorbent material. The nature of the acid and its acidity depend on the material of the ion exchange.

Figure 5.6 shows a schematic representation of an ion exchange process. Ion exchangers are commercially available as enriched beds in tanks. The brine flows downwards into the tank due to gravity. Simultaneously, a second tube injects chemical to adjust the feed's acidity for the best efficiency of the ion-exchanger. The feed solution flows through the ion exchange resin, where the lithium is absorbed, whereas the rest of the filtrate flows outside the tank.

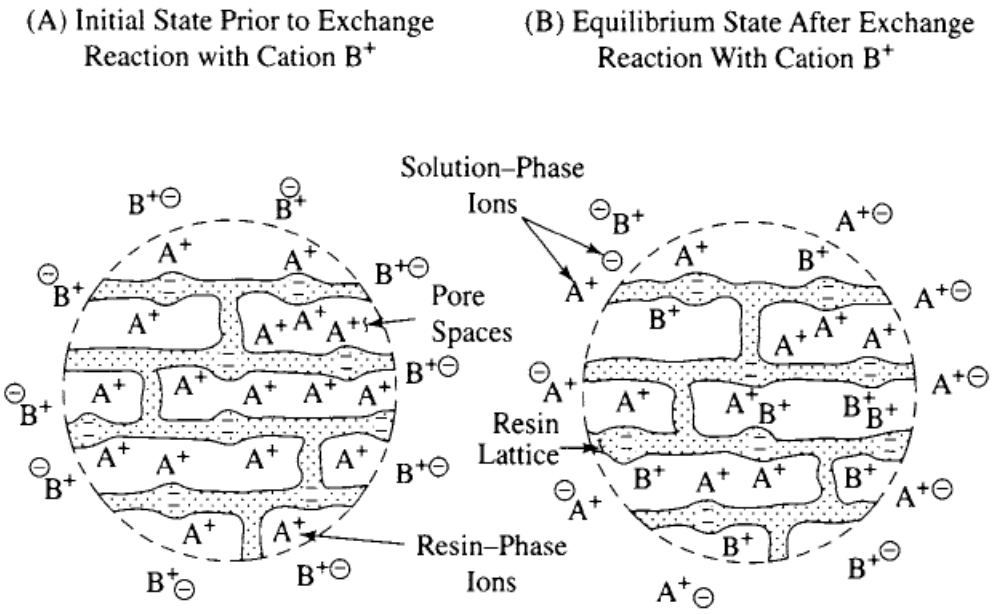

Figure 5.6: Cation exchange resin diagram (Woodard & Currant, 2006). The resin lattice has fixed pore spaces where the exchange reaction occurs. B^+ are the cations initially present in the feed and A^+ the cations initially in the ion exchanger. (A) At the initial state, prior to exchange reactions with the cation B^+, the pore spaces of the resin are filled with the other cation A^+. (B) Once the feed is in contact with the resin and the system reaches the equilibrium, B^+ cations replace the places of A^+ and vice-versa.

Selectivity and Recovery:

Potassium and sodium ions decrease the recovery of lithium. In particular, the potassium ions also influence the permeation process of Li^+ and Mg^{2+} through the resin.

In the economic assessment of E3 Metals Corp. (2021), the company states that with their absorption material the concentration of lithium can increase up to a factor of 11, from 74.6 mg/l up to 850 mg/l.

Zhang et al. (2020), state that the recovery of lithium ranges from 62 to 94.5% for brines with Mg/Li mass ratio respectively from 16.7 up to 400. The higher the mass ration, the higher the recovery according to the research.

Resilience of Material:

Resilience to solids in water

Solid particles limit the efficiency of the method (Woodard & Curran Inc., 2006). The resins have pores of 2/4 mm, so filtration of particles with bigger diameter is expected before the feed enters the ion exchange system.

Resilience to water composition

Ion exchange materials are also generally more selective for higher molecular weight ions. Mg^{2+} cations influence the selectivity of the resin to monovalent ions since they can compete in the lithium's adsorption (Zhang et al., 2020). The ions accumulate on the surface of the membrane creating a positively charged interface, decreasing the lithium recovery. For the separation of lithium, the selectivity of the resin to monovalent cations is as it follows: Ag^{+} >Cs^{+} >Rb^{+} >K^{+} >Na^{+} >Li^{+} (Woodard & Curran inc., 2006).

Some sorbents, such as MnOx and TiOx, are preferentially selective for lithium ions over sodium and potassium, even if these last two are in much higher concentration (Stringfellow & Dobson 2021b). The manganese sorbents are not specified in the Stringfellow & Dobson (2021b) paper, but MnO can be present in the form of MnO^{-2} and MnO^{-4}.

Resilience to temperature fluctuations

Nie et al. (2020) experimentally investigated the extraction of lithium from brines with an ion-exchanger at temperatures between 10 and 30 °C. The higher temperature resulted in lower lithium recovery, as can be seen in Figure 5.7.

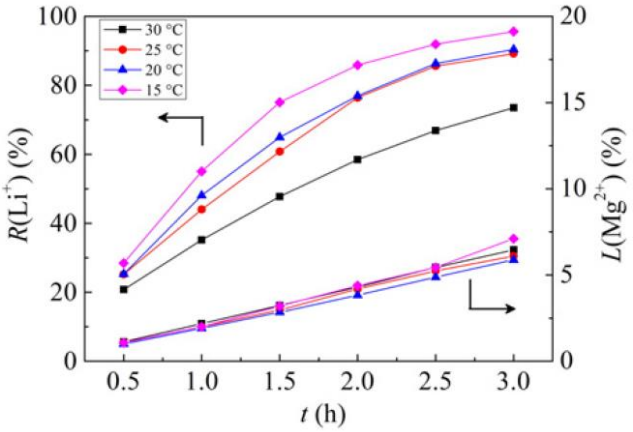

Figure 5.7: Lithium recovery rates ($R(Li^{+})$) compared to magnesium ions as function of time and temperature (Nie et al., 2016).

At higher temperatures, the conductivity of the brine increases, and the leading exchange force becomes electrostatic, where ions with higher electric mass move faster towards the resin. At lower temperatures, the mass transfer of ions is mainly driven by diffusion, and the hydrated ionic radius of the competing cations decreases, making harder the migration of these ions in the material and facilitating the flow of lithium (Yamaguchi et al., 2010 and Nie et al., 2016). Nie et al., (2016) find that lithium recovery at 30°C is 73.5% compared to 95% at 15°C.

Temperature fluctuations of the water can impact the durability of the ion exchange resin since the temperature can influence the equilibrium reactions between elements in the membrane (Nie et al., 2016 and Zhang et al., 2020).

Resilience to flow speed

Nie et al. (2016) analyzes the recovery rate of lithium as function of flow speed in an ion-exchange material. They find that at higher flow speed the recovery rate increases. The increase is a consequence of the turbulent flow at high speeds, that increases the mass transfer of ions rather than the diffusion in the fluid.

Generally, continuous flow ion exchange process is operated from 18 m^3/h to 40 m^3/h for every m^3 of ion exchange resin (Woodard & Curran Inc., 2006).

Ease of sourcing:

This method is used commercially in the final treatment of wastewaters for decontamination and softening of the water. Ion exchangers are also proposed as a primary direct lithium extraction method from geothermal brines (Woodard & Curran, 2006, E3 Metals Corp., 2021 and Toba et al., 2021) since it can be used to recover valuable metals (Zhang et al., 2020 and Stringfellow & Dobson, 2021b).

Space:

Ion exchange resins can work at flow rate of 1.15 m^3/h per m^3 of resin. Hence, at a maximum flow rate of 300 m^3/h in the production part of a geothermal plant, at least 7 m^3 of resin surface would be necessary (Woodard & Curran Inc., 2006). An ion exchange tank is filled only partially with the exchange material. Considering that only half is filled with the exchanger (as schematic drawings of ion-exchangers in Woodard & Curran Inc., 2006), a tank of approximately 14 m^3 is needed for this process at maximum flow speed.

Upstream / Downstream:

The method needs two different phases of acidification, one before the brine flooding and another once the material is fully saturated with lithium. Initially a chemical solution, such as a strong acid solution for the cation extraction, flows through the resin that charges the surface of the material to capture the cations where the anion is mainly chloride (Woodard & Curran Inc., 2006 and E3 Metals Corp, 2021). After the tank is flooded and saturated with metals, the metals removed from the resin by flowing another strong acid by the resin (Nie et al., 2016).

5.1.4. Sorbents

Methodology

Sorbents are solid materials that selectively adsorb specific molecules or ions (Manahan, 1994). The sorbent physically adsorbs LiCl molecules that are recovered by flushing with water, as shown in Figure 5.8 (Wedin & Harrison, 2021 and Stringfellow & Dobson, 2021a). Stringfellow & Dobson (2021a) examinates a series of different sorbent materials for selective lithium extraction.

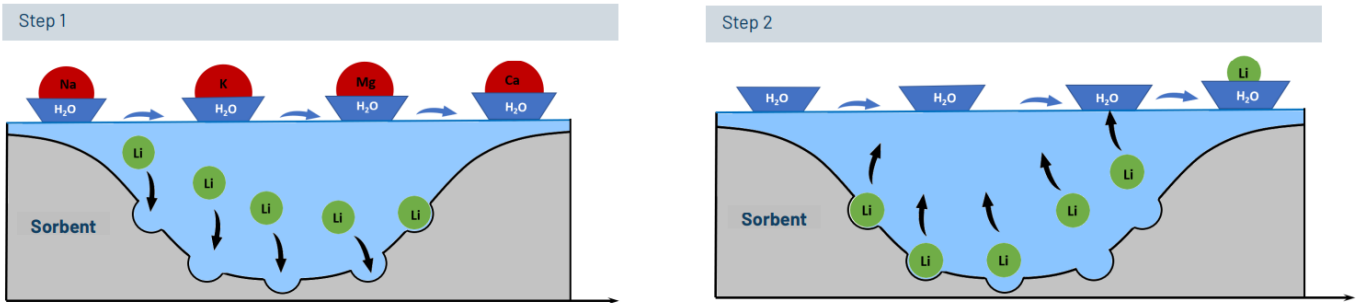

Figure 5.8: Schematic representation of sorption of lithium ions (Wedin & Harrison, 2021).

Selectivity and Recovery:

Wahib et al. (2022) developed a "low-cost and environmentally friendly" adsorbent to remove lithium from groundwater. At pH 6, the sorbent traps 90% of the lithium dissolved in the water. The researchers tested several other sorbents, but the maximum adsorption is 95% with brine at 200 ppm. Another research reported by Sringfellow & Dobson (2021a) states that the lithium recovery achieved is 95%.

Resilience of Material:

The resilience of adsorbent materials varies from the structure and nature of the sorbent (Stringfellow & Dobson 2021a and Wahib et al., 2022).

Resilience to water composition

Adsorption of lithium decreases by 60% at a pH lower than 6. Hydrogen ions in highly acidic solutions compete with the adsorption of lithium ions. Sodium ions can also compete in the adsorption from laboratory experiments on groundwater (Wahib et al., 2022). The adsorption of lithium increases for concentrated brines. Figure 5.9 shows that concentrated brines (100 ppm) result in the maximum adsorption of >95%.

Resilience to temperature fluctuations

It is evident from Figure 5.9 temperature does not play a role in the lithium adsorption capacity. Thus, the sorbent tested can operate at 25 °C, 35 °C, and 45 °C. Differently, Wedin & Harrison (2021) report that one disadvantage of their sorbent material is that the methods need to operate at feed temperatures >50 °C.

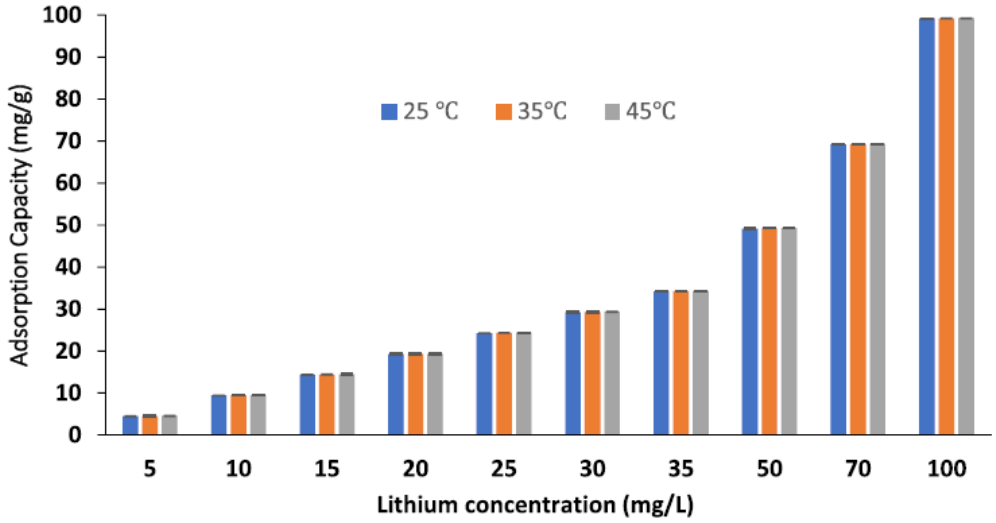

Figure 5.9: Adsorption capacity of sorbent as function of feed concentration and temperature (Wahib et al., 2022).

Ease of sourcing:

Sorbents are widely used to remove trace metals and pollutants from water. The materials are cheaper than membrane filtrations and are environmentally friendly since they do not require the use of additional acidic solutions (Wedin & Harrison, 2021 and Wahib et al., 2022).

Upstream / Downstream:

The pH of the feed needs to be adjusted before the adsorption to acquire an optimal result. The filtrate contains lithium and the competing sodium ions dissolved in water but needs further concentration processes. The lithium concentration in the filtrate can be up to 5 times lower than the feed (from 200 ppm of lithium in the feed to 37 ppm in the filtrate) (Wedin & Harrison, 2021, Stringfellow & Dobson, 2021a and Wahib et al., 2022).

5.1.5. Electrodialysis

Electrodialysis (ED) is a separation process that mobilities ions through a permeable membrane applying an electric field potential on the ion solution. The principle is shown in a diagram in Figure 5.10. The feed solution flows between anode and a cathode of an electrodialysis cell through a series of anion (AEM) and cation (CEM) exchange membranes arranged alternately in the space between the two electrodes (Gmar & Chagnes, 2019; Stringfellow & Dobson, 2021 and Manahan, 1994). Cations pass through the AEM and are retained by the CEM, the opposite happens for negatively charged ions. The process works implementing the adsorption of ion-exchange membranes. Applying an electric field with an anode and a cathode separates ions with same charge and similar ionic radius, such as lithium and sodium.

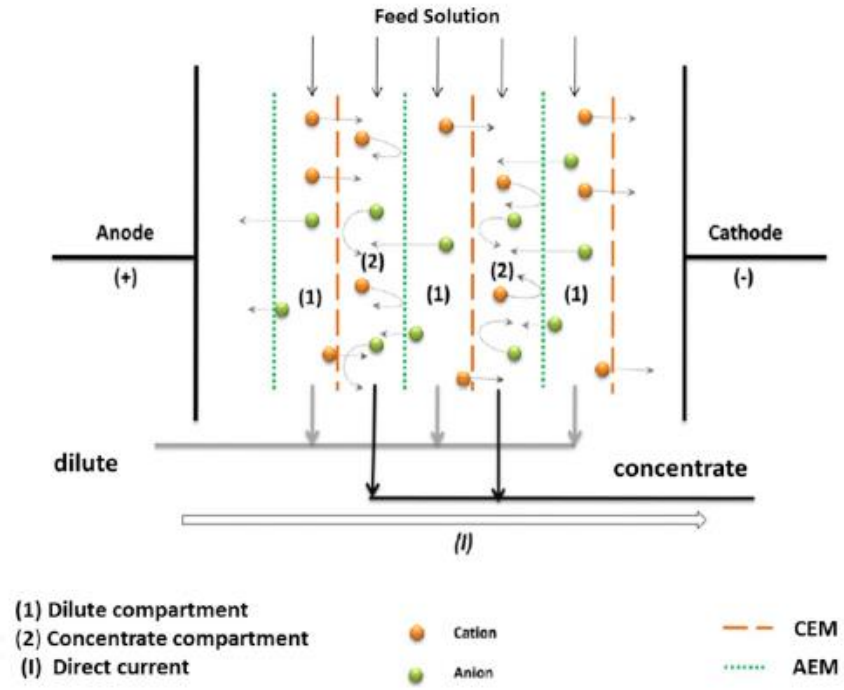

Figure 5.10: Schematic representation of electrodialysis ion separation method (Gmar & Chagnes, 2019).

Selectivity and Recovery:

Gmar & Chagnes (2019) tested the efficiency of lithium extraction from different brine concentrations and found that brines with 1350 ppm of lithium and 27800 ppm of sodium can produce 7650 ppm of LiOH. With a brine containing 700 ppm of Li^+ and 2300 Na^+, the recovery of lithium is only 25%, with an applied electric current density of 0.05 A. However, it can reach 91% if the applied electric current density is 0.1 A. Electrodialysis can be used to purify and produce lithium salts with 95% purity, with a lithium extraction rate of 85%. The average lithium recovery of other experimental setups was 79% (Li et al., 2019 and Ball et al., 1987).

Resilience of Material:

Resilience to water composition

Separation of lithium with electrodialysis lacks when divalent ions or cobalt, nickel and manganese ions are present (Gmar & Chagnes, 2019).

Resilience to temperature fluctuations

Ball et al. (1987) states that the maximum temperature the feed brine can have is of 60 °C. The higher the temperature, the more efficient the ion separation is at the cost of the lifetime of the membranes. The patent specifies that the optimal temperature for the membrane life and efficiency of the system of 30 °C.

Resilience to flow speed

Increasing the flow rate in an electrodialysis extraction plant can positively and negatively impact extraction efficiency. A higher flow rate means higher potential difference, increasing the ion mobility. However, the higher flow rate also decreases the time the feed solution stands in the cell, lowering the recovery of the ions. Electrodialysis extraction plants can operate at flow rates between

14.6 m^3/h and 22 m^3/h (Lee et al., 2019 and Jiang et al., 2014). The maximum flow rate supported by the plant is determined by its manufacturing process.
The recovery rate in electrodialysis cells increases if the current density increases at constant temperature and flow speed. With a concentrated Li^+ of 879 ppm, the final lithium brine has a concentration 400% higher than the initial solution (Jiang et al., 2014).

Ease of sourcing:
ED is used in processes of seawater desalination, treatment of wine and fruit juices, radioactive wastewater treatment and regeneration of ion-exchange resin (Wang et al., 2004).

Space:
Jiang et al. (2014), uses a practical membrane area of 0.01 m^2 to handle the feed brine for lithium extraction at 0.022 m^3/h. For a flow rate of 300 m^3/h, 136 m^2 of membrane is necessary. Commercially available electro deionization modules can be seen in Figure 5.11 (Evoqua Water Technologies, n.d.).

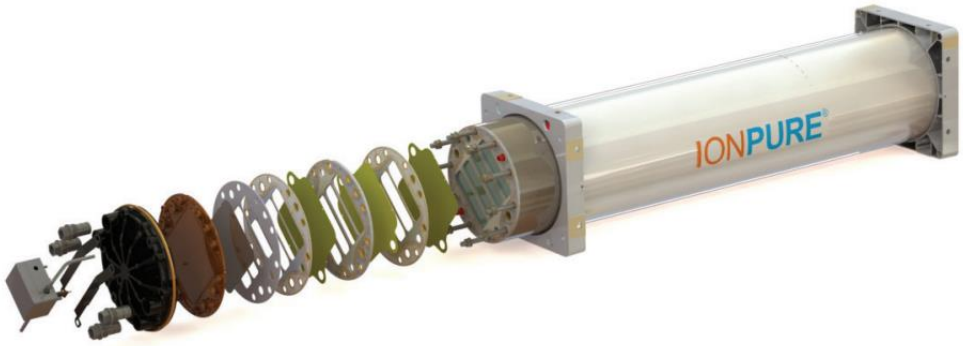

Figure 5.11: Evoqua Water Technologies (n.d.) electrodialyser tube commercially available. The elements displayed are from left to right: pipe adapters, end cap, concentrate spacer, cation membrane,2 dilute spacer, anion membrane, and repeating the sequence of the last four elements.

Upstream / Downstream:
The ED does not require specific acids before the process, but the feed stream needs to be already diluted and removed of most of the metals. The water of some ED facilities needs to flow through a RO filtration process (Lenntech, n.d.).

5.1.6. Summary of methodologies

The separation technologies have limitations and optimal applicability depends on factors such as the feed temperature, flow rate and concentration. In Table 1 the different methods are compared based on some of their requirements. Other factors like the ease of maintaining the extraction facilities can limit the applicability of the methods in lithium recovery from geothermal brines. Other impacting factors can be the composition of the water re-injected in the reservoir, the environmental impact of waste materials, the volume of plant necessary to do the separation of ions and the CAPEX and OPEX of the facility.

	RO membranes	**NF membranes**	**Ion Exchange**	**Sorbents**	**Electrodialysis**
Maximum temperature	45 °C [1, 8]	45 °C [1, 8]	30 °C [6]	>50 °C [15, 16, 17]	30 °C [10]
Operational flow rate	40 m^3/h [13]	1.96 m^3/h [8]	40 m^3/h [7]	*	22 m^3/h [11]
Surface or Volume necessary at flow rate of 300 m^3/h	450 m^3 [2, 8]	462 m^3 [8]	14 m^3 [7]	*	136 m^2 of membrane [11]
Lithium recovery	98-99% [2, 3] Lithium recovered	85% [9]	95% [14]	95% [15, 16, 17]	85% [11, 12]
Permeate	Desalinated brine [1, 2, 5]	Solution with 85% of initial lithium and sodium [9]	Acidified solution with initial salts [6]	Initial brine with 5% of initial lithium [16, 17]	Brine with salts [11, 12]
Concentrate	Concentrated brine with Li^+ and salt ions [1, 2, 5]	Brine with 95% of initial ions and 15% of the initial lithium and sodium [9]	Concentrate solution with 95% initial lithium [6]	Diluted LiCl solution [16, 17]	Highly concentrated LiOH solution [12]

[1] Wang et al. (2004); [2] Porter (1990); [3] Swain (2017); [4] Stringfellow & Dobson (2020b); [5] Wagner (2001); [6] Nie et al. (2016); [7] Woodard & Curran Inc. (2006); [8] Applied Membranes Inc. (2020); [9] Sun et al. (2015); [10] Ball et al. (1987); [11] Jiang et al., 2014; [12] Gmar & Chagnes (2019); [13] Culligan ® (2016); [14] Zhang et al. (2020); [15] Stringfellow & Dobson (2020a); [16] Wahib et al. (2022); [17] Wedin & Harrison (2021)

* Not found in literature

Table 1: Summary of requirements for lithium extraction of the 4 methods analyzed.

* Vulcan Energy Resources: https://v-er.eu/ and E3 Lithium: https://e3lithium.ca/

5.2. Case studies

Two main projects of extracting lithium from geothermal brines have been developed in the last few years by Vulcan Energy and E3 Lithium*. The Vulcan Energy project has passed its FID and from 2024 the company is planning to start the construction of part of the lithium extraction plant (Wedin, 2022), whereas the E3 Lithium has published in September 2021 the Preliminary Economic Assessment of the project (E3 Metals Corp, 2021).

5.2.1. Vulcan Energy: Zero Carbon Lithium ™

Limited data and project plans are available of the project. Some information is protected since some patents still need to be processed by the German government.

Brine composition

The Vulcan Energy project, in Germany, works with brines with similar ion composition of the Dutch geothermal brines (see Appendix A). However, the lithium ions concentrations 4 times higher (200 ppm) than in the Dutch Akkrum-13 aquifer (50 ppm) and almost 5 times bigger than the Californie Geothermie field (40 ppm).

Setup project plant

The company ideated a project divided in three different group of plants: a geothermal plant, a sorption plant and a central lithium plant, as can be seen in Figure 5.12 (Appendix A contains a 3D drawing of the plants) (Wedin & Harrison, 2021).

The geothermal plant used for the project is in Inshem, which is operational since 2012 (BESTEC Unternehmen Zukunftsenergie, 2018). The plant produces up to 28.5 MW of thermal energy and has an average flow rate of 252 m^3/h (Reinecker et al., 2019). A second geothermal plant in Landau which is already operating is planned to be upgraded to produce 360 m^3/h of geothermal brines. During the second phase of the project, five other geothermal power plants will be included, adding 73 MW of electric energy to the energy business. The extraction of lithium from the geothermal brines is planned to happen in two different phases, a sorption plant near the geothermal plant where DLE technologies are applied, and a central lithium plant, for the final refinement processes. Furthermore, the company plans to build one DLE plant on each geothermal plant. Only limited information is publicly available regarding the lithium extraction plants. It is known that a pilot plant is in operation and planned to be scaled up. The company declared the collaboration with DuPont to provide sorbents for the DLE plant (Wedin, 2022), that provided resins to separate the metal (Vulcan Energy Resources, 2022). The pilot plant tested ion exchange resins, but the company is intentioned to use sorbents (Wedin & Harrison, 2021). In Vulcan Energy's annual report of 2021 (Vulcan Energy, 2021b), the company declares that from the pilot plant at bench-scale (10 L scale) the recovery of lithium chloride from the DLE extraction is of 90%. It also states that the "post-treated DLE brine will be materially the same composition as production brine, excluding extracted lithium and silica.". The water with the ions not trapped by the resin is directly re-injected in the reservoir. The recovery of lithium at plant scale or the composition of the re-injected brines are not known at these conditions. However, a video presentation of Vulcan's project (Vulcan Energy, 2021a) shows that lithium is washed from DLE column with water into a "high concentration brine". The annual report states that "the concentration of LiCl concentrate produced from geothermal brine will be further increased using reverse osmosis and mechanical evaporation." (Vulcan Energy, 2021b).

The new concentrated fluid is collected and transported by truck to the separate central lithium plant. They plan to have two or more geothermal plants connected to one central lithium plant. The

extraction and refinement of lithium is planned to be through electrodialysis. Lithium is removed of other impurities and is crystallized to $LiOH.H_2O$ until it reaches the requirements for the battery industry.

Scope of the project:

The economics of the project is divided into two different sections related to the energy business with the geothermal plant, and with the lithium business with sorption plant and central lithium plant. The total CAPEX is €1 738 M, of which 81% is for the lithium business (43% for the sorption plant), whereas the energy business covers only 19% of the plan. It can be argued that the project is a lithium project, not a geothermal energy project.

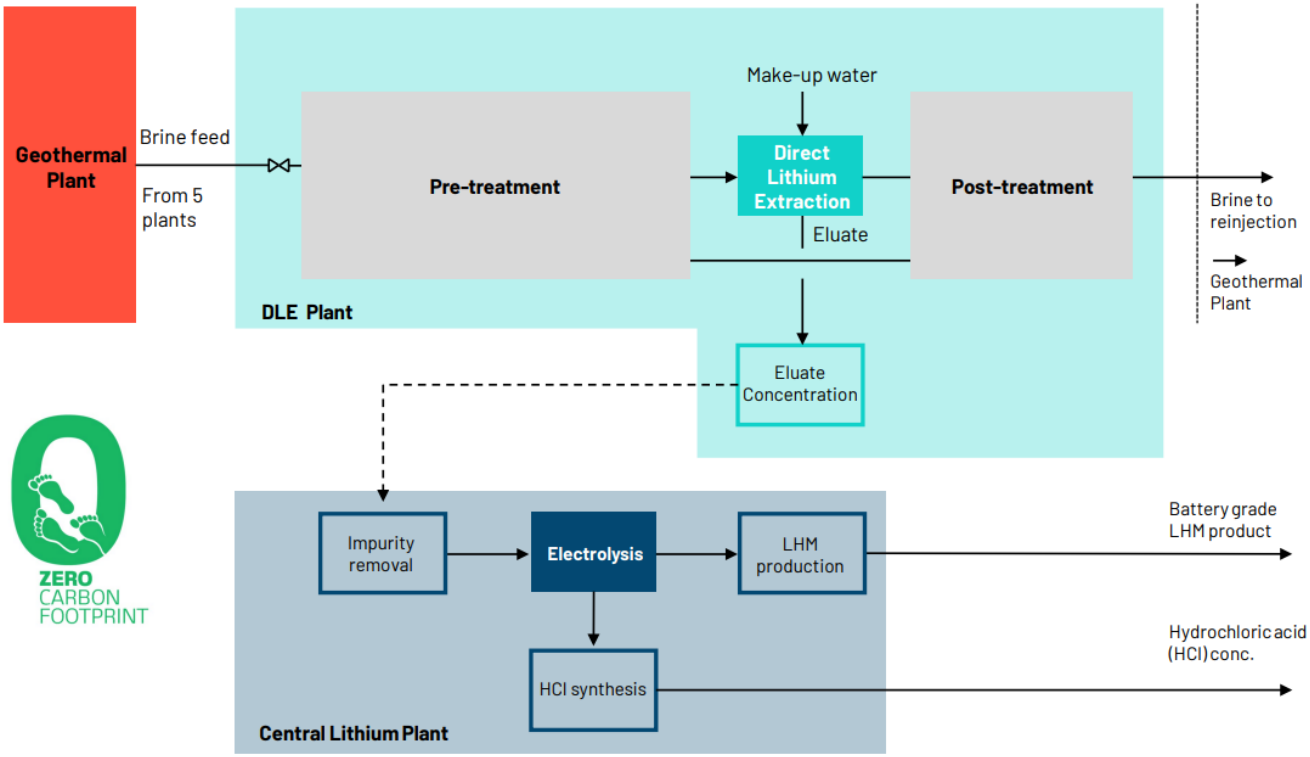

Figure 5.12: Flowsheet of Zero Lithium project from Vulcan Energy (Wedin & Harrison, 2021).

5.2.2. E3 Lithium: Clearwater Lithium Project

Brine Composition

The brines of the project come from the Devonian Leduc Reservoir, a carbonate reef system present in the subsurface of Alberta (E3 Metals Corp., 2017). The lithium concentration is 74.6 ppm.

Setup project plant

The Clearwater Lithium Project does not include a geothermal plant, but it is focusing only on the extraction of brines from the subsurface and the recovery of lithium from them. A schematic block flow diagram of the plant is represented in Figure 5.13 (E3 Lithium, 2022). The brine is extracted from 2500 m depth by deep vertical or deviated wells. Afterwards it is transported to a Central Processing Facility (CPF), by pipelines, where lithium is extracted in two phases. The brine with

concentrated lithium is transported to another facility where it is further refined (E3 Metals Corp, 2021).
The plan includes 2 groups of extraction wells, each composed of 21 wells, to benefit of all the waters in Alberta containing lithium. The wells are expected to produce a maximum of 140 m^3/h each in an overall area of 79 km^2 for 20 years lifetime of the project. The brine extracted from the subsurface is treated to remove solid particles and an ion exchange sorbent oversees the first DLE. The characteristics of the ion exchange resin are unknown, but it is planned to "be formulated into a material which can be used in a fixed bed environment.", recycling the reagent. An example are Resin-in-Pulp and Carbon-in-Pulp vessels. The anolyte solution from the final electrolysis is planned to be used to extract the lithium absorbed in the resin. The company claims that the concentration of the brine from the laboratory-scale DLE plant increases of a factor of 11, from 74.6 ppm to 850 ppm with a recovery of 94% of lithium. The brine released from the sorbent is directly re-injected in the subsurface. The solution containing concentrated lithium is added of lithium carbonate and lithium hydroxide to precipitate calcium and manganese ions. According to the research, these reagents are easily recycled and reused in the processes and do not lead to any significant lithium loss. The lithium solution is concentrated of a factor of 16, in a RO circuit where most of the divalent cations are removed and afterwards the solution is polished through another ion-exchange circuit that lowers even more the divalent cations. It is not specified how much the concentrations are reduced. The final solution is electrolyzed to produce $LiOH.H_2O$ crystals.
The total surface area of the lithium processing plant is of 25900 m^2 and the conceptual plant layout can also be found in Appendix A.

Scope of the project

The project has a total CAPEX of 600 M$ and the payback time (after taxes) is planned to be after 3.4 years. The focus of the project is only to extract lithium and not to use the heat from the subsurface brines. In addition, the project also produces 8.3 m^3/h of fresh water from the RO membranes that can be used for agriculture.

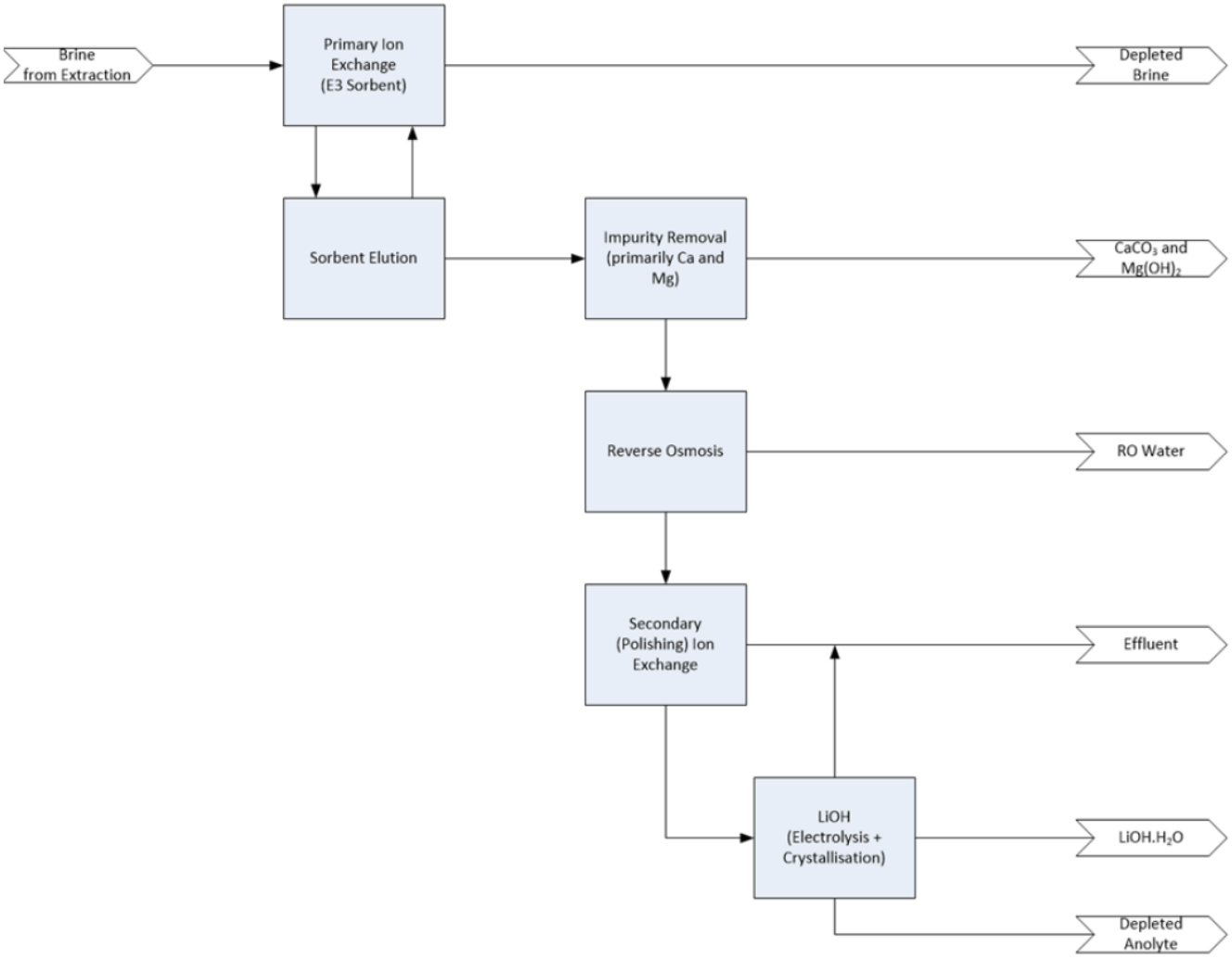

Figure 5.13: Schematic representation of Clearwater Lithium Project (E3 Metals Corp, 2021).

5.2.3. Summary of main differences of the case studies

In Table 2 are briefly explained the main differences of the projects above, to better understand the applicability and re-scaling necessary to future Dutch projects in similar contexts.

	Zero Carbon Lithium ™	**Clearwater Lithium Project**
Brine concentration	181 ppm	74.6 ppm
Plant design	3 different plants	1 plant
Well pads	1 per plant, 2 wells	2, with 21 wells each
Transport Material	Trucks	Pipelines
Flow rate demanded per DLE plant	360 m^3/h	5833 m^3/h

Table 2: Summary of main differences between the Zero Carbon Lithium ™ project and the Clearwater Project.

6

Recommendations on lithium extraction from Dutch geothermal waters

6.1. Likely new operations for lithium extraction based on case studies

The extraction of lithium in both the case studies is planned to happen with similar extraction and purification methods. The brine extracted from the subsurface is concentrated after flowing through a DLE plant. The solution is then transported to another facility to precipitate of other cations, concentrate the lithium with membranes and finally refine the lithium in $LiOH.H_2O$. For lithium extraction in the Netherlands, it is then suggested to investigate a similar approach.

The DLE can occur with ion-exchange resins. The ion-exchange can occur in a vessel of 14 m^3 (Woodard & Curran Inc., 2006), based on 300 m^3/h flow rate, and concentrates the first brines. In this part of the process lithium is adsorbed as well as other cation impurities but leaving most of the anions and divalent and more cations dissolved into the brine. 73.5% of the lithium can be recovered at the operation temperature of 30 °C (Nie et al, 2016). The lithium can be easily separated once the resin is saturated with a strong acidic solution, based on the resin used. The new solution is transported to a second plant where firstly calcium and manganese needs to precipitate, and a RO process eliminates more of the impurities present.
The RO membranes let the water flow through the membrane and block the passage of almost 99% of the remaining ions (Swain, 2017). The membranes are widely used, and they need to operate at high flow speed to allow the reverse osmosis. The projects of Vulcan Energy and E3 Lithium suggest using RO membranes to concentrate the lithium brine. Using an RO membrane, the concentration of other impurity ions increases as well but fresh water is also produced as waste product. All the cations still dissolved in the brine, such as sodium, potassium, and calcium, need to be removed.
A final electrodialysis of the brine can separate the impurities from the lithium, resulting a solution di lithium hydroxide, that is then precipitated in both the case studies in a centrifuge as $LiOH.H_2O$.

Different approaches from the case studies should also be considered. To decrease the costs of the lithium extraction, the Dutch cases might consider improving the lithium separation technologies. Increasing the efficiency of DLE techniques, with higher repulsion for divalent cations can increase the economics of the project. NF membranes could also be considered in the process instead of RO. NF membranes demand less electric energy than RO processes to separate lithium. The filtrate contains in laboratory experiments up to 95% of the initial lithium and can directly flow to the final electrolysis facility. With RO processes the membrane absorbs the lithium and the other ions that are separated in the concentrate. Only with the regeneration of the filter the concentrate leaves the filtration system. Most of ions are still in the concentrate and other processes (such as mechanical evaporation) need to separate the lithium. Moreover, if NF membranes will replace RO, fresh water

would not be produced and that the effluent is a diluted lithium and sodium solution (up to 5 times lower than the feed).

6.2. New operations which require further research

The DLE facility should be placed close to the geothermal wells. The temperature at the outlet of the heat exchanger, after the second filtration, is close to the optimal operational temperature of most of ion-exchange resins. For this, we expect it should be feasible to develop resins operating at 35°C higher, as the temperature of the brine flowing out of the heat exchanger. In addition, the brine that flows through the resin can be directly re-injected in the subsurface without the risk of causing clay swelling. For these reasons, the DLE is optimal to be placed close to the geothermal plants.
The DLE facility, to operate efficiently, needs a minimum flow rate to operate based on the type of facilities used. The Vulcan Energy's project, different to the other case study, plans to use brines from geothermal plants already operating but situated between 5 and 50 km of distance (based on the distances of the Vulcan Energy's project). To maximize the facilities already existent, the project plans to build DLE on the same site of the geothermal power plants. On the other hand, the E3 Lithium's project plans to connect multiple wells to one DLE facility to increase the economics.

Similarly, a centralized DLE facility should be considered in Dutch future projects. Some neighboring Dutch geothermal plants situated in highly agricultural areas, such as the zones close to the Californie Geothermie, might share the same DLE facility. This can be a solution to compensate the lower extraction flow rate compared to the German project. Increasing the amount of production wells delivering at the DLE facility would not impact the delivery of heat to the costumers and would also increase the tonnage of lithium brought at the same plant. Areas where several geothermal plants are already operating and the lithium is present in the brines, can be a first initial step to start researching and investigating the economics of lithium extraction. Centralizing the DLE can be challenging to build pipelines connecting the facility with the injection wells of the original geothermal plants. Not only it is an additional cost to the project, but also it can be tedious to do if the owners of the plants have discrepancies ideas or produce different amount of brines (or with different compositions).

If the DLE facility is centralized in an agricultural area, two problems can be of obstacle to the lithium extraction in a single plant: the size of a combined plant (DLE and lithium refinement) is almost as big as the Colosseum in Rome (25900 m^2, E3 Metals Corp, 2021) and the amount of lithium dissolved might not be high enough to economically refine it. The project of Vulcan Energy to solve these problems plans to build a separate plant for the final refinement and production of lithium monohydrate. Similarly, the Netherlands could build only few refinement plants in strategic locations, reachable by more DLE plants. The German project plans to move the solutions to the final plant by truck, but a solution to reduce transportation costs on the long term might be the construction of pipelines where it is possible. Transportation by trucks is not part of the initial costs since infrastructures such as roads are already highly developed in the Netherlands. However, truck transportation is an additional cost to the OPEX of the project, as well as it increases the CO_2 emissions if normal trucks are used. The construction of pipelines impacts the CAPEX and cannot be built in areas densely populated.

The economics of the solutions above suggested should be further inspected. The scope of the development of lithium extraction projects in the Netherlands can be of improving the economics of geothermal projects, instead of finding a new source of lithium as the two case studies. This helping the local economy and the increasing lithium demand declared by the EU.

6

Conclusion

The value and demand of lithium metal has increased in the past years and is expected to continue growing (Latunussa et al., 2020) mainly because of the need of electric energy storage and the growth of the vehicle industry (U.S. Geological Survey, 2022). To deliver the high demand of lithium developments in finding new sources and extraction methods is necessary.

Lithium in the Netherlands

Europe has in its subsurface potential lithium reserves coming from igneous sources. This research investigates data publicly available on the water composition of the Dutch subsurface from oil and gas projects and geothermal projects.

- Of the water samples lithium is present in higher concentrations in the Californie Geothermie (29 ppm of average Li^+ concentration) and the Akkrum-13 field (47 ppm).
- It is found that no strong correlation between higher lithium concentrations in an aquifer and the specific geological formation: different fields with reservoir rock from same formation as Akkrum-13 have much lower concentrations.
- Moreover, the concentration of lithium is not correlated with the concentration of other elements, despites literature study. Lithium-rubidium concentration graph seems to show a correlation for the R^2 value of 0.94. However, the correlation is based on only 13 samples, not enough to deduct a strong correlation between the metals.
- From geological settings and volcanic intrusions, the lithium seems to come from dissolution and transport along faults of minerals in pegmatitic rocks originated during Rotliegend vulcanisms and close to the German border.

Lithium extraction from geothermal brines

Different methods of extracting lithium from brines have been tested in laboratory scale with methods available in commerce. Some papers (Stringfellow & Dobson, 2021a and Stringfellow & Dobson, 2021b) discuss in detail all experimental methods for the extraction. Wastewater treatment techniques have been developed and available in commerce (Manahan, 1994 and Porter, 1990). Reverse osmosis (RO) and nanofiltration (NF) membranes have been tested in several research for lithium extraction.

- RO resulted in 99% of lithium recovery with no separation from other ions, whereas the NF assures 85% Li^+ recovery with 40% reduction of the concentration of divalent cations. Both the membranes commercially available can operate at feed temperature of 45 °C but need high volumes (450 m^3 and 462 m^3 respectively) and flow speed (40 m^3/h and 1.96 m^3/h) (Wang et al., 2004, Porter, 1990 and Applied Membranes Inc., 2020).
- Ion exchange materials are advanced techniques that requires only 14 m^3 of space at maximum flow speed of 300 m^3/h and the ideal maximum operational temperature is of 30°C for most of the materials. Laboratory experiments tested that the lithium recovery can reach 95% at the ideal

maximum temperature but potassium and sodium ions are also partially adsorbed. The filtrate has only lower lithium, sodium and potassium concentrations, whereas the metal of interest concentrates in the retentate. Other cations can also remain in the concentrate (Nie et al., 2016 and Woodard & Curran Inc., 2006).

- Another filtration method includes sorbents that physically remove LiCl molecules and need only water to recover LiCl adsorbed. The maximum recovery rate is of 95%, with feed brines at >50 °C (Wedin & Harrison, 2021 and Stringfellow & Dobson, 2021a).
- Electrodialysis separates concentrated lithium solutions from impurities still dissolved applying electric current to the feed flowing through a series of ion-exchange membranes. The product is a 95% pure LiOH solution, where 85% of the lithium is recovered (Ball et al., 1987, Jiang et al., 2014 and Gmar & Chagnes, 2019).

Case studies on lithium extraction from brines

Two projects for lithium extraction from aquifer brines are in different phases, Vulcan Energy with the Zero Carbon Lithium™ in Germany and a Canadian project by E3 Lithium named Clearwater Lithium Project. Zero Carbon Lithium™, differently from the other, includes also geothermal power plants in the project.

- The two projects include a direct lithium extraction (DLE) facility close to the extraction brines, followed by central secondary plant where lithium is removed of the impurities and prepared for the commerce (Wedin, 2022, E3 Metals Corp, 2021, Vulcan Energy Resources, 2022 and E3 Lithium, 2022). - A DLE ion-exchange facility, placed after the geothermal plant, followed by a membrane facility to concentrate the brine that is then further polished by the electrodialysis facility.

Recommendation for lithium extraction from Dutch geothermal waters

A different scope more applicable for the Netherlands might be to enhance the economics of geothermal projects instead of making a lithium-based business.

- It is to consider the centralization of the DLE facility in areas where several geothermal projects with lithium prospective are present, such as around the Californie Geothermie. This leads to an increase of brine delivery to the facility and possibly the economic feasibility of the extraction.
- Similarly, the final lithium treatment plant can be centralized and several DLE could deliver their brines to the same facility, as the project of Vulcan Energy.
- To decrease the OPEX costs of transporting the brine by truck as planned by this second case, the construction of pipelines, whether it is possible, can be a solution.
- Further research and developments in increasing the recovery of the metal from the DLE and using efficient nanofiltration membranes instead of reverse osmosis membranes can also be beneficial for the economics of Dutch projects.
- New projects can investigate the areas of Drenthe and Limburg. In the Akkrum-13 area of the Netherlands, there are no geothermal projects operating but only two explorations licenses deliberated from the Dutch government. Retrieving water data of the (old) gas fields are in the area can also improve the knowledge on the lithium composition. Further research and water sampling are necessary in the areas above mentioned to better predict the mobilization of lithium from the source and to further investigate its origin. This, as there is the possibility that some areas closer to the source have higher lithium concentrations than the Akkrum-13 field.

- Lithium extraction techniques are still in the development phase. More membrane filtrations are being tested at laboratory scale and hopefully soon will be available for large scale plants and for a more economical and efficient lithium extraction.

7

Acknowledgments

This report presents my minor research and marks the end of my bachelor's degree on Applied Earth Sciences at TU Delft. I will forever cherish and remember these three years with fond memories. I began this journey of pursuing this bachelor's degree with the support of my family. The passion and devotion they dedicate to their jobs, as well as their sense of curiosity and thirst for knowledge deeply resonated in me. This journey has changed me as a person and has molded me into a better version of myself. This research is the final phase of my journey as a bachelor's student and was made possible by the support of several people. Therefore, I would like to convey my deepest gratitude to them.

Firstly, I would like to thank Pieter Bruijnen (EBN) and Harmen Mijnlieff (TNO) for providing me with their time and the resources necessary to conduct this study. Their help was crucial for the results of the work. I would also like to thank individually also the companies that provided advices and data of their aquifers. Thanks to Wart van Zonneveld (Floricultura), Harmen de Boer, Diederik Westerhof and Tom Covens (Neptune Energy), Annelies Bender (Hydreco Geomec), Peter Csicsovszki (Kistos), Barry Dros (ONE-Dyas B.V.), Nicolaas Boot (TotalEnergies EP Nederland B.V.), Roel van den Ham (TAQA), Koenraad Elewaut (ECW Energy) and Louise Guichelaar.
To continue, I would like to thank my committee for their guidance and constant support throughout the duration of this research. I would like to thank Dr. A.A.A. (Ahmed) Hussain, constantly reassuring me about my work and for pushing me in the right direction. From being a teacher to being my mentor, his support is much appreciated. I would also like to deeply thank Dr. K-H.A.A. (Karl-Heinz) Wolf for his lessons and in-depth feedback during the different phases of this research. His critical analysis of the research has helped me improve the quality of this research as well as the report. I would also like to sincerely thank Dr. M. (Masoud) Soleymani Shishvan that from the beginning was always able to help and insights on topics I had little knowledge before. I am also very grateful to Prof. Dr. D.F. (David) Bruhn, that besides being an inspiration for me could also be part of this project. I would also like to thank Dr. Z. (Zac) Leong for being open to discuss about various topics and provide me insights on technologies I was not aware of. Ahmed Hussain wants also to thank and acknowledge both the sponsorship and advice of RVO, as part of the DIMOPREC project. Finally, I would also like to thank my family and friends who supported me through the entire bachelor by keeping me motivated and helping me to focus on achieving my goals. I will leave my last words to my grandfather, that I am sure is watching over me from wherever he is.

Bibliography

Alley, W.M., Reilly, T.E., Franke, O.L., (2013). *Sustainability of Ground-Water Resources.* U.S. Geological Survey Circular 1186, from https://pubs.usgs.gov/circ/circ1186/html/gen_facts.html

Applied Membranes Inc. (2020). Dupont (DOW) Filmtec membranes. Retrieved 27 July 2022, from https://appliedmembranes.com/filmtec-nanofiltration-membrane-elements.html#details

Ball, L., Boateng, D., Daniel, A.D., (1987). U.S. Patent No. 4,63,295. Method for the recovery of lithium from solutions by electrodialysis

BESTEC Unternehmen Zukunftsenergie. (2018). The Insheim Geothermal Project. Retrieved 1 August 2022, from https://www.bestec-for-nature.com/index.php/en/projects-en/insheim-en

Bradley, D.C., Stillings, L.L., Jaskula, B.W., Munk, LeeAnn, and McCauley, A.D., (2017). Critical mineral resources of the United States—Economic and environmental geology and prospects for future supply: U.S. Geological Survey Professional Paper 1802, p. K1– K21, https://doi.org/10.3133/pp1802K.

Bylund, G., & Tetra Pak Processing Systems AB. (2015). *Dairy processing handbook*. Lund: Tetra Pak Processing Systems AB, from: https://dairyprocessinghandbook.tetrapak.com/chapter/membrane-technology

Culligan ®. (2016). IW EVO Industrial Water. Evolved. Reverse Osmosis. Retrieved from https://www.rwbwater.nl/wp-content/uploads/2019/06/Culligan-IW-Evo-Serie-Omgekeerde-Osmose.pdf

Cunningham, R. E., & Williams, R. J. J. (1980). *Diffusion in gases and porous media*. New York: Plenum Press.

Doornenbal, H., & Stevenson, A. (editors) (2010). *Petroleum Geological Atlas of the Southern Permian Basin Area*. Houten: EAGE Publications b.v.

DuPont. (2022). Industries for Water Treatment & Specialty Separation | Water Solutions. Retrieved 1 August 2022, from https://www.dupont.com/water/industries.html

DutchFiltration. (2018). Geothermal Energy. Applications, Dual vessel filter unit, Equipment. Retrieved 26 July 2022, from https://dutchfiltration.com/geothermal-energy/

E3 Lithium. (2022). Unlocking Alberta Lithium. *Corporate Presentation*. Retrieved from https://static1.squarespace.com/static/61d4d043bad77a1898bc81a2/t/62b4871e6bae976303b6fdf3/1655998241520/2022-06-23-E3+Lithium+Corporate+Presentation_Final.pdf

E3 Metals Corp. (2017). Geological introduction to E3 Metals Corp. Clearwater and Exshaw Lithium-Brine Project in south-central Alberta. Retrieved from https://www.e3lithium.ca/_resources/reports/technical/170518_E3+Metals+Corp_Geo+Intro+43-101.pdf?v=0.664

E3 Metals Corp. (2021). *Preliminary Economic Assessment Clearwater Lithium Project*. Alberta.

Evoqua Water Technologies, (n.d.). IonPure ® Continuous electrodeionization (CEDI) modules. CEDI modules for a wide range of high-purity applications. *Product data sheet.* Retrieved from https://www.evoqua.com/siteassets/documents/products/electrochemical/ion-cedi-br.pdf

Fan, G., Pan, K., Canova, M., Marcicki, J., & Yang, X. (2016). Modeling of Li-Ion Cells for Fast Simulation of High C-Rate and Low Temperature Operations. Retrieved 13 June 2022. doi: 10.1149/2.0761605jes

Flexer, V., Baspineiro, C., & Galli, C. (2018). Lithium recovery from brines: A vital raw material for green energies with a potential environmental impact in its mining and processing. *Science Of The Total Environment*, *639*, 1188-1204. doi: 10.1016/j.scitotenv.2018.05.223

Gao, L., Wang, H., Zhang, Y., & Wang, M. (2020). Nanofiltration Membrane Characterization and Application: Extracting Lithium in Lepidolite Leaching Solution. *Membranes*, *10*(8), 178. doi: 10.3390/membranes10080178

Gmar, S., & Chagnes, A. (2019). Recent advances on electrodialysis for the recovery of lithium from primary and secondary resources. *Hydrometallurgy*, *189*, 105124. doi: 10.1016/j.hydromet.2019.105124

Grotzinger, J., & Jordan, T. (2004). *Understanding Earth* (7th ed.). New York: W. H. Freeman and Company.

Holt, S., Vasmel, M. (2009). *Technisch geologisch onderzoek naar CO_2-opslag in het Barendrecht vled* (Unpublished bachelor's dissertation). Delft University of Technology, Delft, Netherlands.

Jager, J. (2012). The discovery of the Fat Sand Play (Solling Formation, Triassic), Northern Dutch offshore – a case of serendipity. Netherlands Journal Of Geosciences - Geologie En Mijnbouw, 91(4), 609-619. doi: 10.1017/s0016774600000408

Jiang, C., Wang, Y., Wang, Q., Feng, H., & Xu, T. (2014). Production of Lithium Hydroxide from Lake Brines through Electro–Electrodialysis with Bipolar Membranes (EEDBM). *Industrial &Amp; Engineering Chemistry Research*, *53*(14), 6103-6112. doi: 10.1021/ie404334s

Lapperre, R., Kasse, C., Bense, V., Woolderink, H., & Van Balen, R. (2019). An overview of fault zone permeabilities and groundwater level steps in the Roer Valley Rift System. *Netherlands Journal Of Geosciences*, *98*. doi: 10.1017/njg.2019.4

Latnussa, C. E., Georgitzikis, K., Matos, C. T., Grohol M., Eynard, U., Wittmer, D., Mancini, L., Unguru, M., Carrara, S., Mathieux, F., Pennington, D., Blengini, G. A. (2020). *Factsheets on Critical Raw Materials.* European Commission, Study on the EU's list of Critical Raw Materials. doi: 10.2873/631546

Lee, J. (2022). ENERGY minute. Retrieved 12 July 2022, from https://energyminute.ca/single/news/2003/new-battery-life-for-leduc-oil-field

Lee, H., Sarfert, F., Strathmann, H., & Moon, S. (2002). Designing of an electrodialysis desalination plant. *Desalination*, *142*(3), 267-286. doi: 10.1016/s0011-9164(02)00208-4

Lenntech. (n.d.). Mega, RALEX® EDI STACK MPure™ 36. *Product data sheet*. https://www.lenntech.com/Data-sheets/MPure-36-stack-L.pdf

Li, Y., Zhao, Y., Wang, H., & Wang, M. (2019). The application of nanofiltration membrane for recovering lithium from salt lake brine. *Desalination*, *468*, 114081. doi: 10.1016/j.desal.2019.11408

Liu, C., Neale, Z., & Cao, G. (2016). Understanding electrochemical potentials of cathode materials in rechargeable batteries. *Materials Today*, *19*(2), 109-123. doi: 10.1016/j.mattod.2015.10.009

MacEachern, J., & Pemberton, S. (1992). ICHNOLOGICAL ASPECTS OF CRETACEOUS SHOREFACE SUCCESSIONS AND SHOREFACE VARIABILITY IN THE WESTERN INTERIOR SEAWAY OF NORTH AMERICA. *Applications Of Ichnology to Petroleum Exploration*, 57-84. doi: 10.2110/cor.92.01.0057

Manahan, S. (1994). *Environmental Chemistry* (6th ed.). Lewis Publishers.

Medici, G., West, L., & Banwart, S. (2019). Groundwater flow velocities in a fractured carbonate aquifer-type: Implications for contaminant transport. *Journal Of Contaminant Hydrology*, *222*, 1-16. doi: 10.1016/j.jconhyd.2019.02.001

Mercado, A., & Billings, G. (1975). The kinetics of mineral dissolution in carbonate aquifers as a tool for hydrological investigations, I. Concentration-time relationships. *Journal Of Hydrology*, *24*(3-4), 303-331. doi: 10.1016/0022-1694(75)90088-8

Mertineit, M., & Schramm, M. (2019). Lithium Occurrences in Brines from Two German Salt Deposits (Upper Permian) and First Results of Leaching Experiments. *Minerals, 9(12), 766*. doi: 10.3390/min9120766

Nie, X., Sun, S., Sun, Z., Song, X., & Yu, J. (2017). Ion-fractionation of lithium ions from magnesium ions by electrodialysis using monovalent selective ion-exchange membranes. *Desalination*, *403*, 128-135. doi: 10.1016/j.desal.2016.05.010

Reinecker, J., Hochschild, T., Kraml, M., Löschan, G., & Kreuter, H. (2019). Experiences and challenges in geothermal exploration in the Upper Rhine Graben. *Geothermal Engineering Gmbh,*. Retrieved from https://europeangeothermalcongress.eu/wp-content/uploads/2019/07/307.pdf

Porter, M. (1990). *Handbook of industrial membrane technology* (1st ed., pp. 260-305). Westwood: Noyes Publications.

Prices of chemical elements - Wikipedia. (2020). Retrieved 8 July 2022, from https://en.wikipedia.org/wiki/Prices_of_chemical_elements

Salton Sea Simbol Materials. Retrieved 13 June 2022, from http://www.simbolmaterials.com

Schlumberger. (2022). Energy glossary. Retrieved 25 July 2022, from https://glossary.slb.com/en/terms/c/clay_swelling#:~:text=A%20type%20of%20damage%20in,exchange%20or%20changes%20in%20salinity.

Schroot, B. (1991). Structural development of the Dutch Central Graben. *Danmarks Geologiske Undersøgelse Serie B, 16*, 32–35. doi: 10.3997/2214-4609.20140625

Shaw, R.A. (2021) Global lithium (Li) mines, deposits and occurrences (November 2021). British Geological Survey, from https://www2.bgs.ac.uk/mineralsuk/download/global_critical_metal_deposit_maps/G2122_052_V4CMYK.pdf

Sitando, O., & Crouse, P. (2012). Processing of a Zimbabwean petalite to obtain lithium carbonate. *International Journal Of Mineral Processing*, *102-103*, 45-50. doi: 10.1016/j.minpro.2011.09.014

Somrani, A., Hamzaoui, A., & Pontie, M. (2013). Study on lithium separation from salt lake brines by nanofiltration (NF) and low pressure reverse osmosis (LPRO). *Desalination*, *317*, 184-192. doi: 10.1016/j.desal.2013.03.009

Stringfellow,W.T.; Dobson, P.F. (2021). Technology for the Recovery of Lithium from Geothermal Brines. *Energies*, 14, 6805. https://doi.org/10.3390/en14206805, 2021a

Stringfellow, W.T., & Dobson, P.F. (2021). Technology for Lithium Extraction in the Context of Hybrid Geothermal Power. https://pangea.stanford.edu/ERE/pdf/IGAstandard/SGW/2021/Stringfellow.pdf , 2021b

Sun, S., Cai, L., Nie, X., Song, X., & Yu, J. (2015). Separation of magnesium and lithium from brine using a Desal nanofiltration membrane. *Journal Of Water Process Engineering*, *7*, 210-217. doi: 10.1016/j.jwpe.2015.06.012

Swain, B. (2017). Cost effective recovery of lithium from lithium ion battery by reverse osmosis and precipitation: a perspective. *Journal Of Chemical Technology &Amp; Biotechnology*, *93*(2), 311-319. doi: 10.1002/jctb.5332

Syke, J. (2019). *A global overview of the geology and economics of lithium production*. Presentation, Perth.

TNO (n.d.). NLOG, Dutch Oil and Gas portal. Ministry of Economic Affairs and Climate. https://www.nlog.nl/en

Toba, A., Nguyen, R., Cole, C., Neupane, G., & Paranthaman, M. (2021). U.S. lithium resources from geothermal and extraction feasibility. *Resources, Conservation And Recycling*, *169*, 105514. doi: 10.1016/j.resconrec.2021.105514

U.S. Geological Survey, 2022, Mineral commodity summaries 2 022. *U.S. Geological Survey*, 202 p., https://doi.org/10.3133/mcs2022.

Vulcan Energy. (2021a). *Vulcan Energy. Zero Carbon Lithium TM* [Screenshots from Video]. Retrieved from https://www.youtube.com/watch?v=xTMYNfS3RCA

Vulcan Energy. (2021b). *2021 annual report of Vulcan Energy Zero Carbon Lithium ™*. Retrieved from https://annualreport.v-er.eu/wp-content/uploads/vulcan-energy-annual-report-2021-v2.pdf

Vulcan Energy Resources. (2022). *Corporate Presentation*. Presentation. Retrieved from https://v-er.eu/wp-content/uploads/2022/04/Apr-Corp-Preso.pdf

Wagner, J. (2001). *Membrane Filtration Handbook. Practical Tips and Hints* (2nd ed.). Osmonics Inc.

Wang, L., Hung, Y., & Shammas, N. (2004). *Advanced physicochemical treatment processes* (1st ed., pp. 222-280). Totowa: Humana Press.

Wedin, F. (2022). *Vulcan Energy Resources: Vulcan Energy Zero Carbon Lithium™* [PowerPoint slides]. 2022 Corporate presentation. Vulcan Energy Resources Ltd. website: https://v-er.eu/wp-content/uploads/2022/04/Apr-Corp-Preso.pdf

Wedin, F. & Harrison, S. (2022). *Vulcan Energy Resources: Direct Lithium Extraction (DLE)* [PowerPoint slides]. 2022 Technical Update. Vulcan Energy Resources Ltd. website: https://v-er.eu/wp-content/uploads/2021/11/Direct-Lithium-Extraction-technical-update-FINAL.pdf

Wahib, S., Da'na, D., Zaouri, N., Hijji, Y., & Al-Ghouti, M. (2022). Adsorption and recovery of lithium ions from groundwater using date pits impregnated with cellulose nanocrystals and ionic liquid. *Journal Of Hazardous Materials*, *421*, 126657. doi: 10.1016/j.jhazmat.2021.126657

Wong, T., Batjes, D., & de Jager, Y. (editors) (2007). *Geology of the Netherlands* (1st ed.). Royal Netherlands Academy of Arts and Sciences.

Woodard & Curran Inc. (2006). *Industrial Waste Treatment Handbook* (2nd ed., pp. 149-334). Butterworth-Heinemann. https://doi.org/10.1016/B978-075067963-3/50009-6.

Yamaguchi T., H. Ohzono H., M. Yamagami M., K. Yamanaka K., K. Yoshida K., H. Wakita H. (2010). Ion hydration in aqueous solutions of lithium chloride, nickel chloride, and caesium chloride in ambient to supercritical water. *Journal of Molecular Liquids*, 153 (1), 2-8. ISSN 0167-7322. https://doi.org/10.1016/j.molliq.2009.10.012

Zhang, Y. (2010). Diffusion in Minerals and Melts: Theoretical Background. *Reviews In Mineralogy And Geochemistry*, *72*(1), 5-59. doi: 10.2138/rmg.2010.72.2

Zhang, Y., Wang, L., Sun, W., Hu, Y., & Tang, H. (2020). Membrane technologies for Li+/Mg2+ separation from salt-lake brines and seawater: A comprehensive review. *Journal Of Industrial And Engineering Chemistry*, *81*, 7-23. doi: 10.1016/j.jiec.2019.09.002

Appendix A

Data available on lithology and water composition

We are interested in the water compositions of Dutch oil, gas and geothermal aquifers.

Methodology of retrieving data

To retrieve aquifer composition, we use the Dutch government website NLOG (TNO, n.d.), which presents water compositions of Dutch oil, gas, geothermal and salt exploitation projects. TNO kindly provided us with a database of all public compositions.

Type of data available

The water composition reports contain sample details (well details, formation of production, company author of the water report), elements present (ion concentrations) and water properties (pH, resistivity, density).

The samples and the analyses were taken under different conditions and analyzed accordingly to different methods, as indicated in the corresponding water composition reports available on the website. In this analysis we do not consider the influence of the different sampling methods and water analyses that were conducted.

Lastly, some wells are or were producing from multiple reservoirs (commingled completion), thus the produced water has components from multiple reservoirs, without knowing from which formation the water comes from.

Major valuable element present: lithium

Of the data available, only a limited number of samples investigated the presence of valuable metals. Considering a general guideline for the element prices in $/kg ("Prices of chemical elements - Wikipedia", 2020), the element with a higher value and with the highest concentrations found in the Dutch subsurface is lithium.

Figures and tables

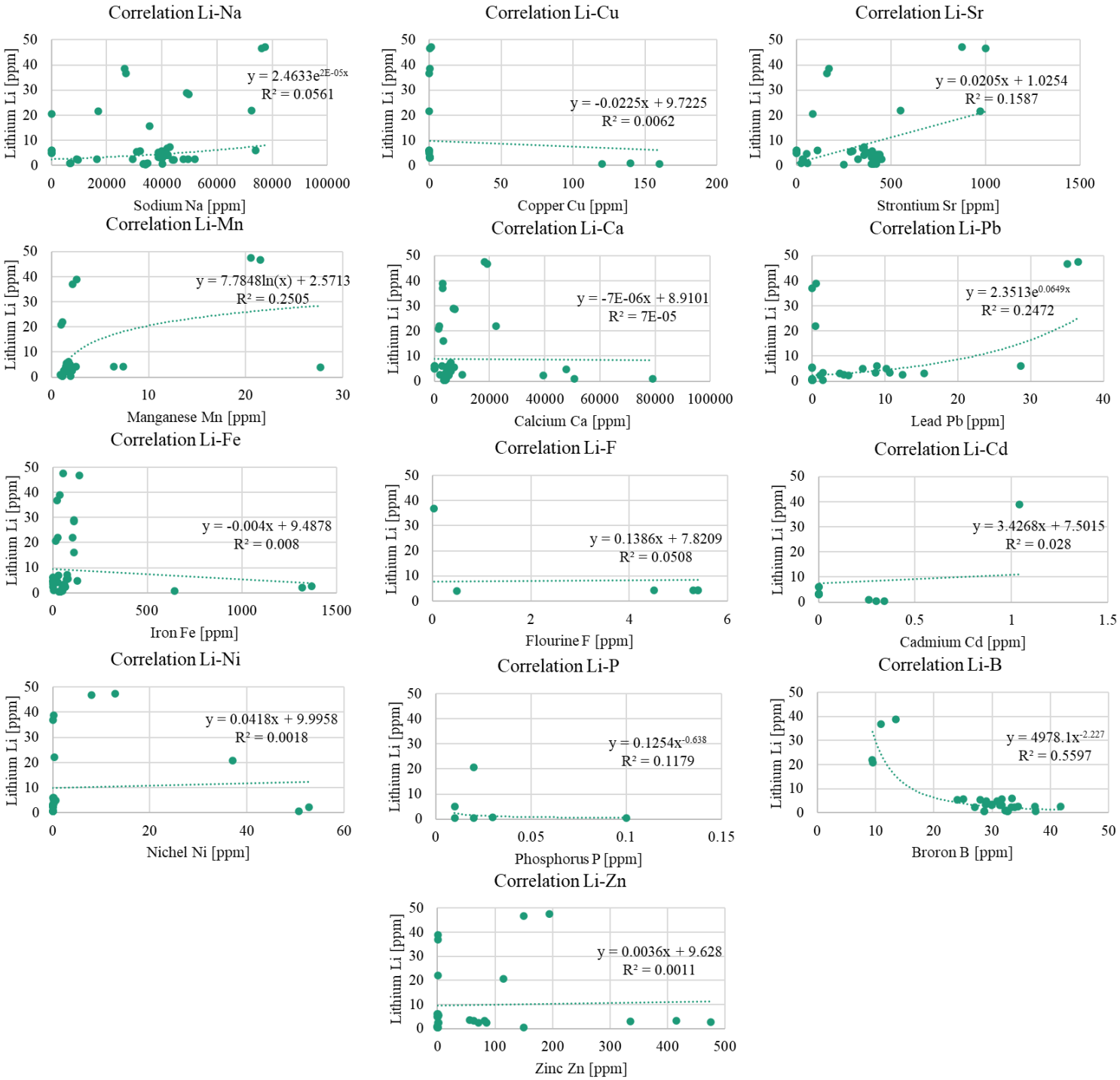

Figure 0.1: Graphs comparing the concentration of different metals with lithium. From top left to bottom right: Li-Na, Li-Cu, Li-Sr, Li-Mn, Li-Ca, Li-Pb, Li-Fe, Li-F, Li-Cd, Li-Ni, Li-P, Li-B, Li-Zn.

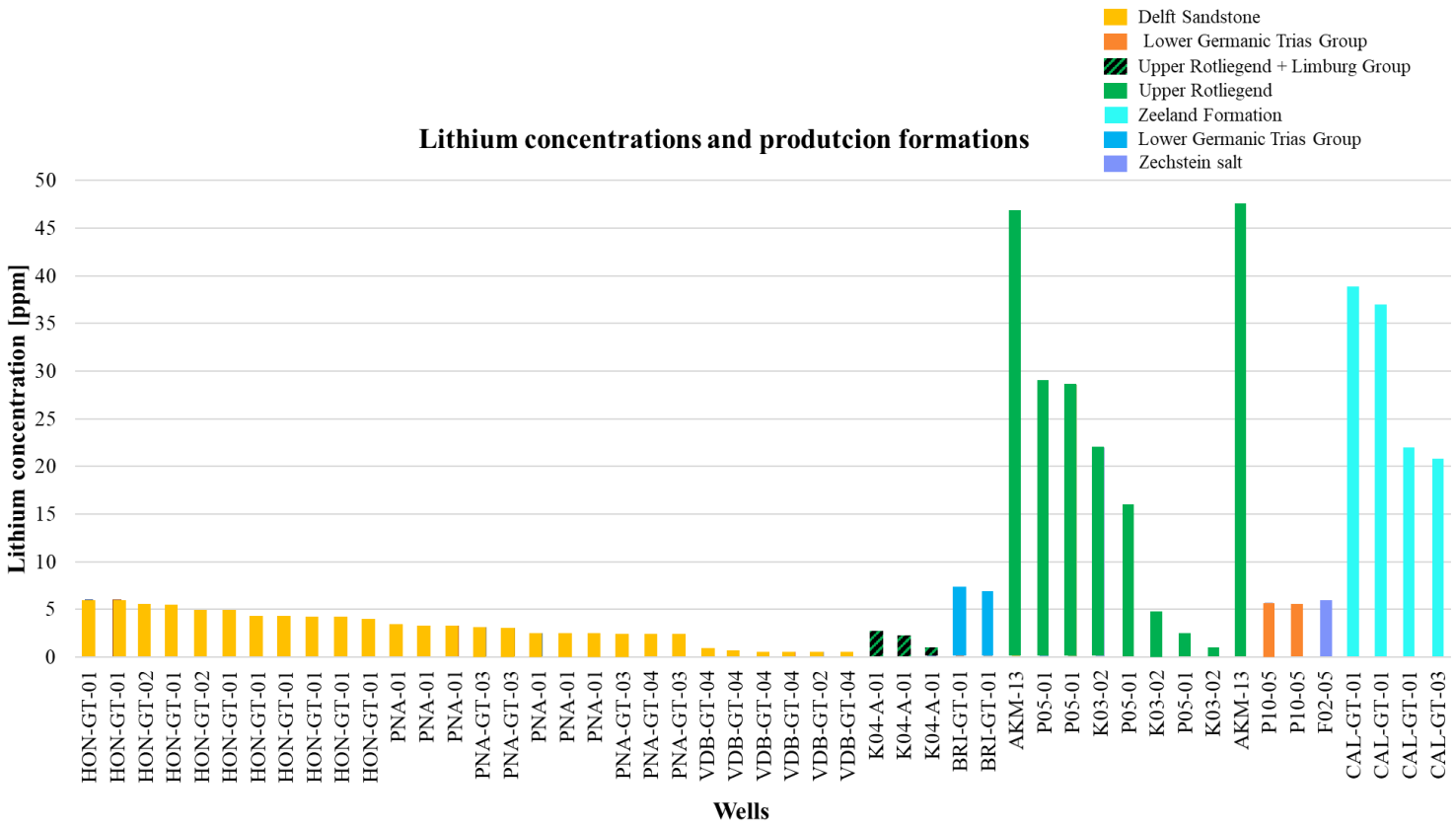

Figure 0.2: All the lithium concentrations available plotted against the well names.

Values	**Units**	Reference
Total average dissolved ions		
879300	**ppm**	TNO (n.d.)
Reverse Osmosis		
1 psi/100ppm		Porter (1990)
8790	psi needed	
60.6	MPa	

Table 3: Calculations for conversion of values from literature.

Short name	units	Na	K	Ca	Mg	Ba	Sr	Fe	Si	Br	Cd	Cr	Cu	F	iI	Li	Mn	Ni	Pb	Zn	B	P	Al	Rb	Cs	Mo	Cl
AKM-13	mg/l	77500	2630	18280	4750	2.1	875	56		312		0.8	1.13		10.7	**47.5**	20.5	12.8	36.5	195			1.3	9.3	2.9		174610
AKM-13	mg/l	76250	1560	19220	2500	8.4	1000	140		314		0.48	0.52		11.5	**46.8**	21.5	8	35	150				10	2.3		175490
CAL-GT-01	mg/l	26459.69	1498	3018	633.2	6.26	172.62	38.7			1.04	0.651	0.17			**38.84**	2.59	0.195	0.57	1.1004	13.425		2	7.835	1.6554		
CAL-GT-01	mg/l	26940	1874	3094	601.4	6.415	160.3	21.81	6.64		-1	0.05	0.05	0.025		**36.92**	2.165	0.1246	0.0214	0.565	10.89		0.1	9.535	1.73		49800
P05-01	mg/l	49000	1590	7010	426			111								**29**											88460
P05-01	mg/l	49700	1580	7310	300			111								**28.6**											**90400**
K03-02	mg/l	72560	1280	22400	1320	6.2	550	105		39						**22**											156140
CAL-GT-01	ppm	17067.69	813.2	1700.76	461.4	9.665	972.2	28.34			-0.2	0.01672	0.04946			**21.98**	1.115	0.3695	0.4788	0.175	9.43		5.04	3.345	0.7652		
CAL-GT-03	ppb / mg/l	16.65	952.9	1588	420	6.1	86.69	15	0.0134		-0.001	- 0.05	- 0.05	-25		**20.75**	1.01	37		115	9.578	0.02		1.46	0.67		*30500*
P05-01	mg/l	35600	1160	3210	61			111								**16**											**58.8**
BRI-GT-01	mg/l	43000	630	5900	900	4.2	356	76								**7.3**							0.5				78000
BRI-GT-01	mg/l	42000	670	5800	880	4.1	350	30								**6.9**							0.5				75000
HON-GT-01	ppb / mg/l	45.87969	0.275	5.18576	1.0778	0.00729	0.4408	0.09494			0.0005	0.01	0.00019			**6.04**	1.77016	0.09581	28.62	0.36	33.445		0.02142	1.07	0.08466	3.14	
HON-GT-01	ppb / mg/l	46.33969	0.2764	5.21976	1.0898	0.00726	0.4446	0.09492			0.00044	0.01128	0.00016 99			**6.03 5**	1.76	0.16	8.84	0.11526			0.295	1.075	0.0845	2.6	
F02-05	mg/l	73910	2180	2732	6907	0.5	110									**6**											145785
P10-05	mg/l	32050	375	4740	820	7.7	295	16								**5.7**					25						59010
HON-GT-02	mg/l	40000	421	7080	894	8.528	399	81	37.7	201		0.0128	0.00383	-0.2	9.9	**5.6**	1.58		0.0156	1.73	31.7						78020
P10-05	mg/l	30960	360	4590	795	6.8	285	5.8								**5.4**					24						60710

HON-GT-01	mg/l	38800	458	6190	983	8.24	373	72.1	50	194		0.01 19	-0.00 75	-1	1	**5.28**	1.67		0.00 81	0.37 2	28		0.00 6			7571 0
HON-GT-02	ppb / mg/l	45.84	0.26 43	5.181	1.03 9	0.00 786 5	0.42 94	0.10 25	0.00 53		-0.00 1		0.00 005	-25		**4.9**	1.87 5	0.59 2	6.9	0.11	30.8 8	0.01	0.1	1.04 5	0.08 23	*84.5*
HON-GT-01	ppb / mg/l	45.96	0.26 7	5.218	1.04 3	0.00 794 5	0.42 89	0.09 3	0.00 934		-0.00 1		- 0.05	-25		**4.89**	1.90 5	0.18	10.2	0.43 5	29.0 4		0.1	1.06	0.84 1	*84.7*
K03-02	mg/l	39595	292 0	4778 0	45	30	54	130		7						**4.7**										1447 20
HON-GT-01	mg/l	42000	270	5900	890	4.4	440	26.3	10.4	181				5.3		**4.3**	6.4									7900 0
HON-GT-01	mg/l	41000	260	5700	880	3.7	430	14.1	9.1	181				4.5		**4.3**	2.5									7800 0
HON-GT-01	mg/l	42000	270	5900	880	5.1	440	0.1	8	168				5.4		**4.2**	1.5									7900 0
HON-GT-01	mg/l	42000	270	5900	890	5.2	440	20.2	8	162				5.4		**4.2**	7.4									7900 0
HON-GT-01	mg/l	42100	269	5890	905	4.3	358	6.7	10.3	199				0.5		**4**	27.7									7800 0
PNA-01	ppb / mg/l	40119.69	208	4393.76	971.4	13.18	406.6	0.155			0.00 03		0.17			**3.42**	1.99 976	0.16	1.46	56.3 6	*29.9 25*		33.2 6	0.92	0.05 368	2.4
PNA-01	ppb / mg/l	38719.69	199.48	4251.76	940.2	12.845	397.6	63.12			0.00 04		0.18 002			**3.3**	1.94 5	0.07 137	10.62	81.34	*28.9 25*		23.9 4	0.90 48	0.05 264	2.02
PNA-01	ppb / mg/l	39579.69	200.2	4327.76	958	13.575	409.8	59.96			0.00 044		0.24			**3.26**	1.95 996	0.12	8.66	415	*29.9 05*		23.68	0.94	0.05 454	2.08
PNA-GT-03	ppb / mg/l	40259.69	214.2	4353.76	994.4	24.34	418.6	54.18			0.00 034		0.16			**3.12**	1.49	0.07 021	3.82	62.7	*31.6 25*		25.68	0.86	0.04 976	3.42
PNA-GT-03	ppb / mg/l	39479.69	211.8	4297.76	978.8	25.26	415.8	54.48			0.00 042		0.26			**3.06 5**	1.48	0.07 361	15.4	335	*31.3 05*		27.8	0.86	0.04 924	2.54
K04-A-01	mg/l	9020	143 0	1008 0	505	0.25	32	137 0		4.9						**2.6**										4418 0
PNA-01	ppb / mg/l	51930	390.1	5245	1213	13.13	451	60.45	0.01 27		-0.00 1		- 0.05	-25		**2.54**	2.11	0.06 94	4.3	475	*34.4 4*			0.90 97	0.05 67	*75.5*
PNA-01	ppb / mg/l	49610	354.9	5100	1165	13.15	437.7	66.7	0.00 431		-0.00 1		- 0.05	-25		**2.505**	2.08 5	0.04 54	12.4	84.8	*41.7 8*			0.9	0.05 57	*78.9*
PNA-01	ppb / mg/l	47740	326	4997	1126	13.14	431.8	65.38	0.00 463		-0.00 1		- 0.05	-25		**2.5**	2.09 5	0.04 42			*37.3*			0.90 5	0.05 56	*80.3*

P05-01	mg/l	16500	700	2000	61									**2.5**											27200
PNA-GT-03	ppm	29387.759	576.5446	5262.8624	825.3714	15.376	325.4902	0.492	7.1266	177.116				**2.43** **733** **86**	1.27689 6008			1.53428 61	27.0754 05						71991.772 18
PNA-GT-04	mg/l	43830	259.1	4646	1055	23.91	424.2	59.63	4.96		-1	-50	-25	**2.33**	1.63	52.7	1.1	70.6	33.32			0.8746	51.2		75500
PNA-GT-03	mg/l	44370	271.7	4699	1068	25.36	429.2	53.35	10.9		-1	-50	-25	**2.3**	1.605	0.0581	5	0.455	33.85			0.873	0.503		77700
K04-A-01	mg/l	9540	1440	39530	460	1.7	36	1320		3.9				**2.2**											85080
K03-02	mg/l	6630	2150	79000	36	23	56	4.3		5.1				**0.95**											144670
VDB-GT-04	mg/l	34859.69	203.2	3713.76	1012.2	36.82	407.2	48.82			0.26	140		**0.91**	0.93	0.06247	0.00318	0.03196	32.225		20.76	0.6096	30.34	2.16	
K04-A-01	mg/l	6890	1320	50800	205	1.7	24	645		1.8				**0.87**											95710
VDB-GT-04	mg/l	40270	295.7	4166	1133	36.51	423	52.9	4.59		-1	-50	-25	**0.69** **5**	1	0.044	0	0	37.45	0.03		0.6131	31.4		66200
VDB-GT-04	mg/l	33299.69	193.78	3539.76	1047.8	28.16	407.6	42.04			0.34	159.84		**0.56**	1.12	0.09335	0.02792	0.445	32.625		27.92	0.56	21.86	2.44	
VDB-GT-04	mg/l	33279.69	195.28	3531.76	1046.2	27.88	403.6	41.18			0.3	120		**0.55** **5**	1.11	0.11017	0.00374	0.14	32.665		28.44	0.4896	21.44	2.04	
VDB-GT-02	mg/l	*34280*	*168.9*	*3631*	*1052*	*27.94*	*402.2*	*41.63*	10.3		-1	-50	-25	**0.54**	1.15	50.6	1.5	149.6	28.63	0.01		0.4796	21.1	0	62900
VDB-GT-04	mg/l	34330	163.2	3621	1043	27.38	396.3	34.42	5.93		-1	-50	-25	**0.49**	1.14	0.05046	0.00016	0.30049	28.61	0.02		0.475	20.9	0	62100
HAG-GT-01	mg/l	34000	970	3900	1000	7.2	250	33	8.3		0.01	0.13		**0.45**	2					0.1					81000

Table 4: Table with metal concentrations of Dutch fields (TNO, n.d.).

		Upper Rhine Valley Brine	Salton Sea Brine	URV vs SS
Salts (Cations)	Analyte	Mg/kg Value	Mg/kg Value	%
Lithium: Source of revenue	Li	214	213	+1%
	Na	22,231	59,600	-63%
	K	4,878	18,126	-73%
	Rb	30.0	-	
	Cs	16.0	-	
	Mg	99	54	+83%
	Ca	5,195	31,714	-84%
	Sr	276	475	-42%
	Ba	14.4	139	-90%
Anions				
	Cl	60,567	145,000	-58%
	SO4	172	127	+35%
	F	4.7	24	-81%
	Br	288	-	
Metals (Cations)				
Requires additional purification step if high	B	47	401	-88%
	Be	0.0207	0.2	-91%
Can negatively affect DLE if high	Si	67.2	550	-88%
Can negatively affect DLE if high	As	20.3	8.8	+131%
Can negatively affect DLE if high	Mn	24.5	1,563	-98%
Can negatively affect DLE if high	Fe	37.4	664	-94%
Can negatively affect DLE if high	Zn	5.2	492	-99%
	Pb	0.156	108	-100%
Can negatively affect DLE if high	Al	0.014	16	-100%
	Ni	0.188	0.5	-61%
Can negatively affect DLE if high	Co	0.015	8	-100%
	Sb	0.717	6.5	-89%
	Ti	<0.1	-	
	V	0.165	0.6	-71%
	Cr	0.181	2	-89%
	Cd	0.0205	3	-99%
	Mo	0.0124	8	-100%
	Tl	0.328	2	-86%
pH		5.828	4.9	

Figure 0.3: Geothermal brine compositions of Upper Rhine Graben and Salton Sea Brine (Wedin, 2022).

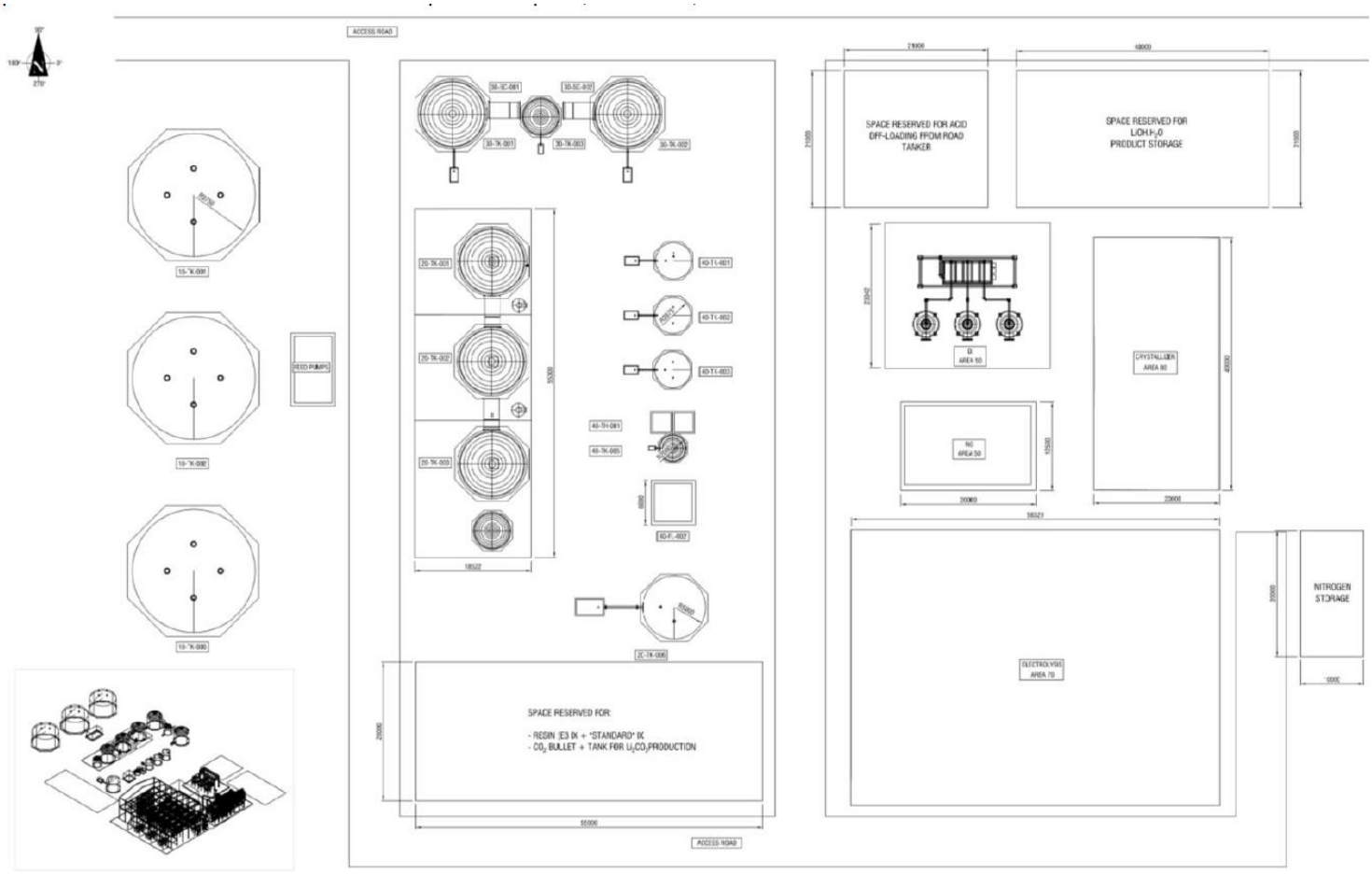

Figure 0.4: Conceptual layout of the lithium processing plant (E3 Metals Corp, 2021).